

1 Author Response: Referee comments (requirement 1) are followed by in-line author responses
2 (requirement 2) denoted by “AR,” and followed by any relevant changes in the text (requirement
3 3).

4
5 Interactive comment on “Investigating types and sources of organic aerosol in Rocky Mountain
6 National Park using aerosol mass spectrometry” by M. I. Schurman et al.

7 **Anonymous Referee #1**

8

9 This manuscript reports the characterization of submicron aerosols with an Aerodyne
10 HR-ToF-AMS at a remote site in the Rocky Mountain National Park (RMNP) in summer
11 2010. By applying PMF to the organic aerosol mass spectral data, the authors identified three OA
12 factors, including a low volatility OOA that correlates with sulfate, a semivolatile OOA that
13 correlates with nitrate, and a local BBOA that shows enhanced signal at m/z 60 and 73 in the
14 factor mass spectrum and appeared to be related to campfire burning. The sources of the particles
15 at RMNP are discussed based on particle composition, size modes, and meteorological
16 measurements. The authors also mentioned that the results of this study appear to be
17 representative of typical summer-time condition at this location according to historical
18 measurement data in this region.

19 This work provides important, new information about aerosol chemistry and sources at a
20 background site in the Front Range area. The work is carefully conducted and the manuscript
21 well written. The scope of the work also fits well to ACP. I thus recommend publication on ACP
22 after the authors respond to the following comments.

23

24 A main portion of this manuscript deals with organic factors determined from PMF analysis of
25 the AMS organic matrix and the usage of this information to interpret aerosol sources. However,
26 some aspects of the PMF results are questionable. For example, the Q/Q_{expected} values (Fig. S1)
27 are much lower than 1, suggesting an overestimation of the errors.

28

29 AR: Thank you for your rigorous reading! Yes, this error overestimation is explored in the
30 supplement (pp. 2/line 28 – pp. 3/line 17), following error propagation from signal-error
31 determination in the data acquisition through downweighting during PMF analysis; we have
32 expanded this discussion somewhat based on your comments.

33

34 The SV-OOA and BBOA factors are very similar, in terms of both mass spectra and time series.
35 A large fraction of the m/z 60 and 73 signals goes to the SV-OOA factor. All of these suggest
36 factor mixing. Recombining factors from the solution of a larger number of factors seems
37 promising, but more information should be given. It is important to show the mass spectra and
38 time series of the 6 factors and offer details on how the recombination was performed. How do
39 the BBOA* calculate from recombining the 6-factor solution compare to BBOA from the 3 factor
40 solution?

41

42 AR: Thank you for your feedback; some of this information was shown in the supplement, and
43 this section has now been expanded. Additions include: mass spectra (MS) and time series (TS)
44 for 6-factor solution (Figure S3), with correlation coefficient (r) values between the factors' TS
45 and MS; an explanation of how the six factors were recombined into three; coefficients of
46 determination (r²) between recombinant *BBOA, *SV-, and *LV-OOA and inorganic species

1 (Table S1) and between recombinant factors' mass spectra (Table S2); and more extensive
2 comparison of the original and recombinant BBOA factors.

3
4 Detailed comments:

5
6 The abstract and the summary both make references to historical measurement, it will helpful to
7 give some details.

8 AR: Citations, data types and sources, and relevant statistics for comparison with historical data
9 are described in Table 1; the caption has been revised to include more methodological details for
10 the historical measurements.

11
12 Page 19878, Line 1, replace Zhang et al. 2005 with Zhang et al., 2011.

13 AR: Done; thanks for your feedback.

14
15 Page 19879, line 9 -10, it says "a DMPS study-average submicron size distribution shows that the
16 AMS aerodynamic lens transmits _ 98.7% of submicron mass". What is 98.7% corresponding to?
17 How was this determined? Note that the AMS lens transmission is size dependent.

18 AR: Yes, we took into consideration the size dependence of AMS lens transmission. We
19 multiplied the volume distribution from the DMPS (analogous to mass assuming constant particle
20 density, but in any case the units cancel) by the aerodynamic lens transmission function, and
21 divided that by the DMPS volume distribution (Liu et al., 2007); this assumes that our
22 instrument's lens transmission function is the same as that of Liu et al.'s instrument.

23
24 Page 19880, give information about how CPF is performed.

25 AR: Page 19880, Lines 8-10 give the method of calculation and the threshold used for filtering
26 (thresholds were applied using a mask wave in IGOR, but could be accomplished similarly in any
27 number of programming languages). We included this information in text instead of equation
28 format to save some space.

29
30 Page 19880, line 22, saying that the sulfate "timeline less featured" is vague. Please be specific.

31 AR: Thank you; it now reads, "Sulfate concentrations are lower and less variable..."

32
33 Page 19909, Figure 5, it will be interesting to add the ratios of other elements too, e.g.,
34 C/H, C/N.

35 AR: Thank you, this has been done.

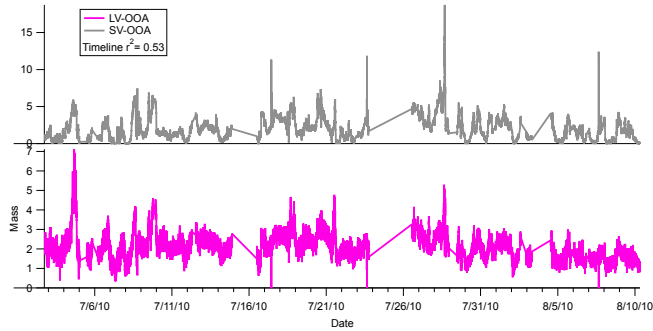
36
37 Page 19883, line 22 -25, the logic is not clear – why is the fact that S(VI) species result from
38 S(IV) oxidation the reason that particles containing sulfate have been subject to advanced
39 oxidation?

40 AR: This has been reworded; we mean merely that, while it is certainly possible for S(VI) to
41 partition to a less-oxidized particle, contemporaneous transport (and attendant oxidation) of S-
42 species and organics will tend to yield highly oxidized organics in concert with S(VI), as has been
43 observed in numerous ambient datasets.

44
45 Page 19884, line 3-4, if thermal partitioning is the reason for LV-OOA increase at night, why
46 nitrate does not show the behavior? In fact, all OA factors increase at night, suggesting a BB

1 influence that “contaminates” the OOA factors.
2 AR: The increase at night is observed in sulfate, ammonium, and nitrate diurnal profiles as well.
3 This was alluded to in Page 19881, line 15, but has now been rewritten to be explicit.
4
5 Page 19885, line 26, what does “arbitrary” mean?
6 AR: Under the dictionary definition, “arbitrary” is not precisely the right word, as it implies a
7 distinction made without logic or reason, and SV- and LV-OOA do have explicit definitions in
8 the AMS community (namely, which of m/z 43 or m/z 44 contains more signal, respectively).
9 The point we are trying to make is not that the definitions of SV- and LV-OOA are technically
10 arbitrary, or that semi- and low-volatility material don’t behave differently/have different sources,
11 but that ambient aerosol oxidation varies continuously such that a particle subject to oxidation
12 may, at a given time, be defined as ‘SV-OOA,’ while by the next time step the same particle may
13 technically be ‘LV-OOA’; under such circumstances, the delineation between SV-OOA and LV-
14 OOA – purely in terms of oxidation (as stated in the text) - do not indicate a major difference in
15 particle source or content. The next sentence goes on to describe how differentiation in sources
16 can be determined from associations between differing levels of oxidation and inorganics,
17 meteorology, etc. We are merely stating that oxidation level as measured by m/z43/m/z44 is
18 somewhat fluid and, by itself, incomplete indicator of sources and processing.
19
20 Page 19886, the organic nitrogen results are very interesting. It might be interesting to report the
21 comparison of the AMS total CHN signal to the total WSON measurements from PILS, e.g.,
22 correlation coefficient and scaling factors etc.
23 AR: Unfortunately, we have only weekly filter-based PM2.5 PON measurements; these
24 comparisons may be explored in the future.
25
26 Page 19889, line 9-10, it is helpful to show the size distribution image results in the
27 supplementary.
28 AR: This figure will be included in revisions to the supplement.
29
30 Figure 5, the huge m/z 29 peak in the BBOA factor is strange.
31 AR: We have noted ‘unusually’ high signal at m/z 29 in all of the datasets gathered using this
32 instrument; after exploring possible causes in the data analysis processes, peak fitting, ion
33 choices, etc. appear to be correct (i.e. the signal is real), so we must conclude that our instrument
34 tends to fragment more than others; it is established in the literature that fragmentation for various
35 species is inconsistent between instruments (as discussed in, e.g. Farmer et al., 2010).
36
37 Figure 10, the purple trace on NO₃ plot is hard to see.
38 AR: The blue (NO₃ data) trace is now somewhat lighter for greater contrast; thank you for noting
39 this.
40
41 Figure S3, how do the time series of the two OOA factors derived from data with f₆₀<0.003 look
42 like? What are their correlation behaviors with nitrate and sulfate?
43 AR: The timelines are included below; they resemble the SV- and LV-OOA timelines from the 6-
44 factor recombinant solution. As shown in the table below, they retain the pattern of better
45 correlation between LV-sulfate and SV-nitrate, as in the other solutions, though the coefficients
46 of determination are weaker (like those in the 6-factor recombinant solution). This information is

1 omitted from the main text and supplement for brevity, but is part of the public record in the form
2 of this communication.



3

	SV-OOA'	NO ₃	SO ₄	NH ₄
LV-OOA'	0.53	0.35	0.46	0.38
SV-OOA'		0.46	0.23	0.30

4
5
6 Figure S4, is this the solution of PMF performed on the entire org. matrix?
7 AR: yes; the captions are now more specific.

8
9 Thank you again for your comments.
10 Investigating Types and Sources of Organic Aerosol in Rocky Mountain National Park Using
11 Aerosol Mass Spectrometry
12 Referee #2 Comments

13
14 Author Response: Please see in-line responses denoted by “AR:”

15
16 Comments

17
18 The authors nicely discuss the chemically speciated AMS data measured at the Rocky
19 Mountain National Park between the 2nd of July and the 31st of August 2010. The organic fraction is
20 deconvolved by the means of the positive matrix factorization algorithm (PMF), presented and mainly
21 discussed within the manuscript. The authors also speculate based on scientific criteria about the
22 presence of organonitrates (ON) and about the role of biogenic SOA most probably present in SV-
23 OOA and LV-OOA.

24
25 AR: Thank you for your review and useful feedback!

26
27 I am most concerned about the fact that the BBOA and the SV-OOA profiles are still mixed up, as
28 already recognized and stressed by the authors. This is also evident from the fact that both profiles
29 and are quite similar, if one neglects m/z 29 in the BBOA mass spectrum. Moreover, the time series
30 of these two factors do also co-vary to some extent. Along this line, it would be beneficial for the
31 reader to have a table containing the correlation values for the time series among the factor time
32 series.

1
2 AR: This information is available in Figure S1(b). Also, the supplement is now revised to contain
3 more statistics on the recombinant PMF solutions.
4
5 As emphasized by the authors, BBOA and SV-OOA are not completely unmixed (similarity of the
6 profiles, ts-covariation, O:C ratio). The authors realized the importance of the exploration of the
7 solution space, by performing the fpeak analysis, exploring higher numbers of factors and testing the
8 PMF solutions excluding strong BBOA events. Unfortunately, the fpeak analysis is too unspecific and
9 failed to retrieve an unmixed solution. The attempt of exploring a higher number of factors bears a
10 high potential and to my knowledge, it was already tested and published for the AMS-Montseny data
11 (see Crippa et al., 2014 and reference therein). I would suggest to rather either use the cleaner BBOA
12 profile retrieved with such a technique. For the reapportionment of the secondaries I recommend to
13 either regroup accurately the other profiles into the respective SV-OOA and LV-OOA families, or to
14 constrain the obtained clean BBOA profile in a 3-4 factor solution employing the ME-2 algorithm
15 (see the recent study of Canonaco et al. 2013). In addition, I was wondering if some minor
16 contribution from the Colorado Hwy 7 road might be expected too? If so, and assuming that the
17 authors are willing to test the ME-2 solver, I would also suggest to constrain the local traffic profile in
18 order to estimate the advected traffic contribution from the surroundings.
19 I recommend this article to be published in ACP after a cleaner BBOA profile is extracted and the
20 discussion part is updated accordingly.
21

22 AR: Thanks for your feedback. New *BBOA, *SV-OOA, and *LV-OOA from recombination of a 6-
23 factor PMF solution were presented in the supplement. We did perform all of the above-suggested
24 analyses (save using ME-2), and those results were included in the supplement, which now includes
25 more detail, such that the two types of solutions (original and recombinant) are independently
26 interpretable. Though we have also noticed that recombinant factors are gaining legitimacy in the
27 literature (and, thank you for the additional citations), the recombinant factors yield the same
28 (qualitative, in both cases) information about the types and temporal variability of aerosols affecting
29 the site; taking into consideration the support from the other referee for expansion of recombinant-
30 solution detail in the supplement and retention of the original solution in the main text, it seems not
31 inappropriate to use the original solution in the main text.

32 As to contributions from Hwy 7, we saw no evidence of periods with HOA-like aerosol in, for
33 instance, the van Krevelen diagram (Figure 6). Given that Hwy 7 sees very light traffic and is
34 removed from the sampling site by ~200 m and a vegetative barrier, it is unsurprising that traffic
35 signal is not evident, given PMF's inability to resolve factors contributing <5% of mass.
36

37

38

39

40

41

42 |

1 **Investigating Types and Sources of Organic Aerosol in Rocky Mountain National**
2 **Park Using Aerosol Mass Spectrometry**

3

4 M. I. Schurman¹, T. Lee^{1,2}, Y. Sun^{1,3}, B. A. Schichtel⁴, S. M. Kreidenweis¹, J. L. Collett, Jr.¹

5 [1]{Department of Atmospheric Science, Colorado State University, Fort Collins, CO}

6 [2]{Now at Department of Environmental Science, Hankuk University of Foreign Studies, Seoul,
7 South Korea}

8 [3]{Now at State Key Laboratory of Atmospheric Boundary Layer Physics and Atmospheric
9 Chemistry, Institute of Atmospheric Physics, Chinese Academy of Sciences, Beijing, China}

10 [4]{National Park Service/CIRA, Colorado State University, Fort Collins, CO}

11

12 Correspondence to: M. I. Schurman (mishaschurman.ms@gmail.com)

1 **Abstract**

2 The environmental impacts of atmospheric particles are highlighted in remote areas where
3 visibility and ecosystem health can be degraded by even relatively low particle concentrations.
4 Submicron particle size, composition, and source apportionment were explored at Rocky
5 Mountain National Park using a High-Resolution Time-of-Flight Aerosol Mass Spectrometer.
6 This summer campaign found low average, but variable, particulate mass (PM) concentrations
7 (max = $93.1 \mu\text{g}/\text{m}^3$, avg. = $5.13 \pm 2.72 \mu\text{g}/\text{m}^3$) of which $75.2 \pm 11.1\%$ is organic. Low-volatility
8 oxidized organic aerosol (LV-OOA, 39.3% of PM_1 on average) identified using Positive Matrix
9 Factorization appears to be mixed with ammonium sulfate (3.9% and 16.6% of mass,
10 respectively), while semi-volatile OOA (27.6%) is correlated with ammonium nitrate (nitrate:
11 4.3%); concentrations of these mixtures are enhanced with upslope (SE) surface winds from the
12 densely populated Front Range area, indicating the importance of transport. A local biomass
13 burning organic aerosol (BBOA, 8.4%) source is suggested by mass spectral cellulose
14 combustion markers (m/z s 60 and 73) limited to brief, high-concentration, polydisperse events
15 (suggesting fresh combustion), a diurnal maximum at 22:00 local standard time (LST) when
16 campfires were set at adjacent summer camps, and [association with](#) surface winds consistent with
17 local campfire locations. The particle characteristics determined here represent typical
18 summertime conditions at the Rocky Mountain site based on comparison to ~ 10 years of
19 meteorological, particle composition, and fire data.

20 **1. Introduction**

21 From alpine meadows to stark peaks, Rocky Mountain National Park (RMNP) hosts abundant
22 wildlife, an important water catchment, and roughly 3 million visitors per year (Annual Park
23 Visitation Report, NPS Public Use Statistics Office). Recent studies chronicle visibility reduction
24 in RMNP, a Clean Air Act Class I protected environment, due to fine particles, especially in the
25 summer when concentrations are higher (Levin et al., 2009; Malm et al., 2009**b**). Environmental
26 impacts from increased nutrient - and particularly nitrogen - deposition are also documented in
27 the Colorado Rocky Mountains (Baron et al., 2000), where mountain-valley circulations
28 periodically transport ammonium, nitrate, and other particulate species from agricultural and
29 urban sources to the east (Benedict et al., 2013[a&b](#)). However, organic compounds contribute the

1 majority of fine-particle mass and attendant visibility impairment at RMNP during summer
2 months (average July 1991-2006 PM_{2.5} organic mass fraction = 51 ± 6%, Levin et al., 2009);
3 unfortunately, beyond indications that contemporary carbon (denoting biomass burning and/or
4 biogenic VOC condensation) and organic nitrogen contribute to organic mass (Benedict et al.,
5 2013a; Schichtel et al., 2008), local organic aerosol (OA) types and sources are unknown. In fact,
6 studies concerning remote environments are infrequent despite the myriad health, environmental,
7 and climate effects of fine particles (Solomon et al., 2007) and the fact that such sites comprise
8 the atmospheric ‘background’ that contextualizes our developing understanding of atmospheric
9 chemistry. Those that do exist indicate a range of particle sources from transported urban
10 particles (e.g. Sun et al., 2009) to biomass burning (e.g. Corrigan et al., 2013) and secondary OA
11 formation involving biogenic VOCs (e.g. Chen et al., 2009); efficient mitigation strategies clearly
12 require a sophisticated understanding of OA sources.

13 This study explores particle sources and composition at a remote site in Rocky Mountain
14 National Park during 2 July-31 August 2010 as part of the Rocky Mountain Atmospheric
15 Nitrogen and Sulfur (RoMANS) Study. The Time-of-Flight Aerosol Mass Spectrometer (HR-
16 ToF-AMS or ‘AMS’) analyzes submicron, non-refractory particles quantitatively for size and
17 composition with high mass- and time- resolution (Decarlo et al., 2006); Positive Matrix
18 Factorization (PMF) is used to deconvolve a matrix containing 2-5 minute average organic mass
19 spectra into a number of spectrally-static organic ‘factors’ whose contributions to total organic
20 mass vary over time (Paatero & Tapper, 1994).

21 PMF-derived factor mass spectra (MS) may reveal particle sources through comparison with MS
22 profiles of various compounds and aerosol types (Alfarra et al., 2007; Lanz et al., 2007; Zhang et
23 al., 2011). Correlating factors with inorganic tracers by particle size and concentration may also
24 support source identification (Zhou et al., 2005). For instance, biomass burning organic aerosol
25 (BBOA) may be identified by fragments of levoglucosan (C₆H₁₀O₅) and other anhydrosugars -
26 products of cellulose and hemi-cellulose combustion - in the ambient mass spectra at *m/z* 60
27 (C₂H₄O₂⁺), *m/z* 73 (C₃H₅O₂⁺), etc. (Simoneit et al., 1999; Weimer et al., 2008); BBOA is
28 sometimes, but not always, correlated with potassium (K), another known combustion tracer
29 (Echalar et al., 1995; Sullivan et al., 2008).

30 Other common classifications are based on organic compounds’ degrees of oxidation.
31 Hydrocarbon-like Organic Aerosol (HOA) is produced chiefly by fuel combustion and

ms 10/22/14 4:28 PM

Deleted: IPCC

ms 10/23/14 7:26 PM

Comment [1]: This citation should be Zhang et al., 2011 (instead of Zhang et al., 2005); the citation is already in the reference list.

1 distinguished by hydrocarbon chains at m/z 57 ($C_4H_9^+$, Lanz et al., 2007; Zhang et al., 2005). The
2 spectrum of Semi-Volatile Oxidized Organic Aerosol (SV-OOA or OOA-II) is characterized by
3 the predominance of hydrocarbons and/or carbonyls at m/z 43 ($C_3H_7^+$ or CH_3CO^+) over more
4 oxidized fragments at m/z 44 (mostly CO_2^+ , Lanz et al. 2007; Ulbrich et al. 2009). Lastly,
5 enhanced signal at m/z 44 indicates highly oxidized Low-Volatility Oxidized Organic Aerosol
6 (LV-OOA or OOA-I, Lanz et al. 2007; Ulbrich et al. 2009); oxidized OA is often observed in
7 rural and remote areas (Zhang et al., 2007). Using particle composition with factor analysis,
8 particle size, and meteorological data, this work constructs a comprehensive description of
9 submicron particle sources and suggests, through comparison to historical data, that these
10 represent 'typical' summer conditions at Rocky Mountain National Park.

11 2. Methods

12 Particles were sampled in a valley on the SE side of Rocky Mountain National Park at ~2740 m
13 (Lat: 40.2778, Long: 105.5453; Figure 1). The sampling site is adjacent to the Salvation Army
14 High Peak, Covenant Heights, Timberline, and Aspen Lodge Resort camps, but removed from
15 urban centers and considered rural; traffic on the nearby Colorado Hwy 7 is light. The AMS was
16 co-located with meteorological, CASTNet, and IMPROVE (designator: ROMO) stations, a
17 particle-into-liquid sampler (PILS-IC, Orsini et al., 2003), Hi-Vol filter samplers, URG annular
18 denuders, a differential mobility particle sizer (DMPS; TSI 3085), an optical particle counter, an
19 aerodynamic particle sizer, and an automated precipitation sampler. Beem et al. (2010), Levin et
20 al. (2009), and Benedict et al. (2012) present results from measurements using some of the above
21 instrumentation. Rigorous AMS calibration and data quality assurance protocols were used,
22 including weekly or bi-weekly ionization efficiency calibrations and HEPA filtration periods. For
23 this study, a DMPS study-average submicron size distribution shows that the AMS aerodynamic
24 lens transmits ~98.7% of submicron mass (Ezra Levin, personal communication, 22 November,
25 2011; Liu et al., 2007). Data analysis utilized SQUIRREL (v1.51H), PIKA (v1.10H, Sueper et al.,
26 2011), and the PMF2 algorithm (Paatero & Tapper, 1994) in PET (v2.03A, Ulbrich et al., 2009) in
27 Igor Pro 6.22A (WaveMetrics Inc., Lake Oswego, OR). Elemental analysis of high-resolution
28 mass spectra utilized the updated AMS fragmentation table for ambient OA in Aiken et al.
29 (2008). Data preparation for the PMF analysis followed Zhang et al. (2011) and Ulbrich et al.
30 (2009) and included fragments m/z 12-110; solutions for 1-5 factors were explored with varying

ms 10/22/14 4:33 PM

Deleted: 2013

ms 10/22/14 4:34 PM

Deleted: ≤

1 rotational parameters ($-1 \leq \text{FPEAK} \leq 1$, in increments of 0.2). A three-factor solution was
2 selected based on criteria presented in Ulbrich et al. (2009) and Zhang et al. (2011), as discussed
3 in more detail in Section 3.2. Diagnostic information for this PMF solution can be found in the
4 supplement, along with 2- and 4-factor solutions (Figures S1, S5, and S6).

5 Chemical source apportionment is often supported by meteorological information; many studies
6 have used wind direction, HYSPLIT, and other back-trajectory products to map source regions
7 and transport (Chan et al., 2011; Sun et al., 2010). Here, complex flow over mountainous terrain
8 produces back-trajectories that may be useful in aggregate but lack the specificity needed to study
9 individual events (Gebhart et al., 2011); fortunately, links between increased NO_x concentrations
10 and low-level upslope flow from the Front Range indicate that less complex meteorological
11 analysis may aid source apportionment (Parrish et al., 1990). Thermally-induced afternoon
12 upslope (NE-S, 45° - 180°) and nighttime downslope (SW-N, 225° - 360°) winds are well
13 established in the Rocky Mountains and may transport urban plumes toward or away from the
14 RMNP site, respectively (Figures 1 and 2; Bossert & Cotton, 1994); the co-located ROMO met
15 station records hourly surface observations.

16 The Conditional Probability Function (CPF) identifies wind directions contributing high
17 constituent concentrations and is well supported in the literature (Kim & Hopke, 2004; Xie &
18 Berkowitz, 2007); the CPF equals the number of concentration points greater than a threshold
19 (here, the concentration average plus one standard deviation) measured in a given wind sector
20 divided by the number of data points in that sector.

21 3. Results

22 3.1 General Particle Composition and Concentration

23 Submicron aerosol mass concentrations during these summer measurements were fairly low, with
24 an average (\pm one sd) of $5.13 \pm 2.72 \mu\text{g}/\text{m}^3$, and comparable to average $\text{PM}_{2.5}$ measurements from
25 the IMPROVE network during July and August from 2005 to 2012 ($5.13 \pm 4.36 \mu\text{g}/\text{m}^3$, CIRA
26 2013). Total organics dominate with frequent higher-concentration events manifested in both
27 brief, high-amplitude spikes, and longer-duration, lower-intensity increases (max. = $93.1 \mu\text{g}/\text{m}^3$,
28 avg. $3.86 \pm 2.66 \mu\text{g}/\text{m}^3$, Figure 3); organics contribute $75.2 \pm 11.1\%$ of total non-refractory
29 submicron mass on average, which is consistent with the organic contribution to 24-hour average

ms 10/23/14 7:27 PM

Deleted: S2

ms 10/23/14 7:27 PM

Deleted: S3

ms 10/22/14 4:35 PM

Deleted: td dev

ms 10/22/14 4:36 PM

Deleted: ,

1 PM_{2.5} found in the summer of 2006 ($60 \pm 12\%$; Hand et al., 2012; Levin et al., 2009). Sulfate
2 concentrations are lower and less variable (max. = $7.45 \mu\text{g}/\text{m}^3$, avg. $0.85 \pm 0.48 \mu\text{g}/\text{m}^3$); nitrate
3 and ammonium concentrations are also low on average but with some higher concentration
4 episodes (Figure 3, NO₃: max. = $5.37 \mu\text{g}/\text{m}^3$, avg. $0.22 \pm 0.24 \mu\text{g}/\text{m}^3$; NH₄: max. = $2.05 \mu\text{g}/\text{m}^3$,
5 avg. $0.20 \pm 0.14 \mu\text{g}/\text{m}^3$). These values are statistically similar to concentrations in previous
6 datasets covering 2005-2012, showing low inter-annual variability in major species and total
7 particulate mass (Table 1). Time-series correlations indicate ammonium-nitrate ($r^2 = 0.89$) and
8 ammonium-sulfate ($r^2 = 0.97$) mixtures; ammonium nitrate and ammonium sulfate commonly
9 arise in ambient particles produced from ageing of agricultural, industrial, and other
10 anthropogenic sources. The low correlation between nitrate and sulfate ($r^2 = 0.34$, Table 2) may
11 indicate that they are not regularly internally mixed in the local aerosol. Formation mechanisms
12 and/or upwind source types and locations for particulate ammonium nitrate and ammonium
13 sulfate may differ: ammonium nitrate may arise from reaction of gaseous nitric acid and
14 ammonia, while the presence of sulfate may reflect in-cloud or gas phase oxidation of sulfur
15 dioxide (Barth et al., 2000; Lelieveld & Heintzenberg, 1992; Seinfeld & Pandis, 2006); this will
16 be explored further in following sections.

17 Diurnal average concentration patterns are shown in Figure 4. Nighttime increases in inorganics
18 may be caused by thermal partitioning and/or boundary layer compression, and mirror those seen
19 in oxidized OA PMF factors, as discussed later. Diurnal means of inorganic species increase
20 sharply in the afternoon, in contrast to the 25th and 75th percentiles, which are similar in profile to
21 the oxidized organics (next section); this indicates that the mean values are influenced
22 disproportionately by fewer, high-concentration events and may not indicate 'typical' behavior.
23 The afternoon increases in the means of sulfate and ammonium have a pattern different than that
24 of nitrate, supporting the suggestion that events and/or mechanisms driving concentrations of
25 ammonium sulfate differ from those influencing nitrate. Nitrate has a bi-modal mean similar to
26 total organics and presaging the organic nitrogen content explored in Section 3.3. Concentrations
27 of total organics and all inorganic species begin to increase at ~10:00-12:00 LST, approximately
28 2-4 hours after the ~8:00 LST initiation of upslope winds (Figure 2), consistent with typical lags
29 observed in episode analysis (Section 3.7).

ms 10/23/14 7:29 PM

Comment [2]: Changed to, "Sulfate concentrations are lower and less variable (...)" instead of "sulfate concentrations are lower and their timeline less featured (...)"

ms 10/23/14 7:31 PM

Comment [3]: After "Fig. 4." inserted the sentence, "Nighttime increases in inorganics may be caused by thermal partitioning and/or boundary layer compression, and mirror those seen in oxidized OA PMF factors, as discussed later."

1 3.2 PMF-Derived Organic Aerosol Factors

2 The selection of number of PMF factors is based on factors' spectral and timeline dissimilarities,
3 comparison to 'established' factor types, and correlation with tracers such as inorganic species.
4 The supplement to this work details the PMF analysis. Positive Matrix Factorization suggests a
5 three-factor solution with Biomass Burning Organic Aerosol (BBOA, Figure 5; Simoneit et al.
6 1999) and two types of oxidized organics, Low-Volatility Oxidized Organic Aerosol (LV-OOA)
7 and Semi-Volatile Oxidized Organic Aerosol (SV-OOA; Lanz et al. 2007; Ng et al. 2010) as
8 defined in the introduction. All of these factors are quite oxidized, with oxygenated fragments
9 often dominating signal at a given m/z (note fragment families $C_xH_yO_1$ and $C_xH_yO_{n>1}$ in Figure 5)
10 and significant CH_3CO^+ (at m/z 43) and CO_2^+ (at m/z 44).

11 PMF solutions are subjective since they involve qualitative user inputs such as number of factors;
12 indeed, we hypothesize that some 'BBOA' mass may be misallocated to the SV-OOA factor by
13 the algorithm. The most compelling evidence is that the SV-OOA mass spectrum contains some
14 m/z 60 and m/z 73, but average mass spectra of all high-SV-OOA periods with no commensurate
15 increase in BBOA do not contain mass at m/z 60 and m/z 73 (Fig. S4); therefore, an SV-OOA
16 mass spectrum containing these biomass burning markers does not represent the vast majority of
17 elevated-SV-OOA periods.

18 Secondly, timeline and meteorological data indicate that the OOA factors are transported with
19 inorganics from the Front Range (Section 3.5); dilution during transport tends to yield gradual,
20 sustained, and moderate (~2-3 times average) concentration increases (Fig. 3). The appearance,
21 then, of brief, high-amplitude SV-OOA events commensurate with BBOA but not with
22 inorganics is inconsistent with the likely behavior of transported, aged SV-OOA (see example:
23 period A, Fig. 11). This is not conclusive, of course, as real increases in particulate SV-OOA
24 could also arise from semivolatile organic carbon (SVOC) condensation onto the newly available
25 biomass burning particle surface area. However, diurnal patterns echo these timeline
26 idiosyncrasies; the 22:00 LST increase in BBOA is mirrored in the diurnal modes of m/z 60 and
27 SV-OOA (Fig. 4), but in a PMF run excluding periods with BBOA events (defined as $f_{60}>0.003$,
28 the ambient background), SV-OOA increases only slightly at night and is similar to LV-OOA in
29 amplitude and pattern (Fig. S4). Apportionment of some BBOA mass to SV-OOA would account
30 for enhanced m/z 60 mass in the SV-OOA mass spectrum and the increased SV-OOA
31 concentration during BBOA events.

ms 10/22/14 6:48 PM

Deleted: Figure

ms 10/23/14 7:31 PM

Deleted: S3

ms 10/22/14 6:49 PM

Deleted: Figure

ms 10/22/14 6:49 PM

Deleted: Figure

ms 10/22/14 6:49 PM

Deleted: Figure

ms 10/22/14 6:49 PM

Deleted: Figure

ms 10/23/14 7:32 PM

Deleted: S3

1 In PMF, the FPEAK parameter is used to explore linear transformations, or ‘rotations,’ of the
2 solution matrix that redistribute mass between the factors, presenting alternate solutions (Ulbrich
3 et al., 2009). Positive FPEAK allocates less m/z 60 and m/z 73 to SV-OOA and more to BBOA,
4 but also re-allots mass at other m/z s to BBOA; this renders the BBOA time line increasingly like
5 that of SV-OOA, which is unphysical because it suggests that BBOA increases during periods
6 when no biomass burning markers are present in the mass spectra, as explained above. A six-
7 factor solution with subsequent recombination to three factors produced better-resolved BBOA
8 and SV-OOA factors (Fig. S2), for which increases in f_{60} are commensurate with increases in
9 BBOA but not with SV-OOA (Fig. S2). This solution produced the conclusions, as above, that
10 LV-OOA is associated with ammonium sulfate, SV-OOA with ammonium nitrate, and BBOA
11 has sporadic, high amplitude events (Table S1). However, since this recombination technique is
12 more subjective, and yields the same conclusions about the local aerosol, the original 3-factor
13 PMF analysis with FPEAK=0 is presented here. The LV-OOA factor is generally most abundant
14 (average = $2.15 \pm 1.11 \mu\text{g}/\text{m}^3$), and features longer duration (~6-11 hour), low amplitude (2-3
15 times average) elevated-concentration events. The LV-OOA time series is correlated with sulfate
16 and ammonium (Table 2), similar to studies with LV-OOA factors from anthropogenically-
17 influenced secondary aerosol formation (Zhang et al., 2011). Internal mixing of sulfate and low-
18 volatility OA may arise from similar oxidation pathways; the advanced oxidative processing that
19 produces low-volatility OA will also tend to produce S(VI) if S(IV) species are present in the
20 same air mass (Jimenez et al., 2009). For instance, aqueous processing is known to efficiently
21 produce both low-volatility organic compounds and S(VI) species.

22 The LV-OOA factor increases consistently in the afternoon (diurnal mean mode at 14:00-15:00
23 LST) and nighttime (mode at 22:00 LST, Fig. 4). The afternoon increase may arise from transport
24 with upslope winds, as will be explored later; the nighttime concentration maximum begins to
25 form at ~16:00 LST, when temperatures start to drop (Fig. 2), which may indicate effects from
26 boundary layer compression and/or thermal partitioning. Both OOA factors also feature a subtle
27 8:00 LST minimum, which could be attributed to thermal boundary layer expansion before an
28 influx of particles associated with afternoon upslope winds.

29 While the SV-OOA factor is lower in general, it is more variable (average = $1.51 \pm 1.63 \mu\text{g}/\text{m}^3$);
30 the SV-OOA timeline is punctuated by longer duration, low amplitude concentration increases
31 similar to (and often accompanied by) LV-OOA increases, but also short, high-amplitude (4-10

ms 10/22/14 6:49 PM

Deleted: Figure

ms 10/23/14 7:32 PM

Deleted: S6

ms 10/22/14 6:49 PM

Deleted: Figure

ms 10/23/14 7:33 PM

Deleted: , untested in the literature,

ms 10/23/14 7:35 PM

Comment [4]: Replaced "S(VI) species result mainly from atmospheric oxidation of S(IV) species, and thus particles containing sulfate have been subject to advanced oxidative processing, which also tends to produce low-volatility OA " with "the advanced oxidative processing that produces low-volatility OA will also tend to produce S(VI) if S(IV) species are present in the same air mass"

ms 10/22/14 6:49 PM

Deleted: Figure

ms 10/22/14 6:49 PM

Deleted: Figure

1 times average, max. = $64 \mu\text{g}/\text{m}^3$) periods commensurate with increasing BBOA as discussed
2 above. Like LV-OOA, SV-OOA has two modes in the diurnal average; however, the evening
3 increase is more pronounced than that of LV-OOA (from misallocation of BBOA, as discussed
4 above). SV-OOA is correlated with ammonium and, more weakly, nitrate (Table 2), suggesting
5 influence from urban areas and/or agriculture.

6 The BBOA factor is generally very low (average $0.46 \pm 0.21 \mu\text{g}/\text{m}^3$), but has brief (~1-2 hour),
7 higher-concentration episodes; these events occur in the evenings and the occasional afternoon,
8 producing a consistent diurnal mode at ~22:00 LST commensurate with nighttime campfires at
9 adjacent summer camps and an outlier-driven mean increase at ~16:00 LST (Fig. 4, High Peak
10 Camp manager Russ Chandler, personal communication, 9 September 2012). BBOA is not
11 correlated with other AMS-determined aerosol components or 17-minute PILS-IC potassium ($r^2 =$
12 0.01); however, the K^+ timeline periodically tracks BBOA. Because K^+ is emitted mainly during
13 the fire flaming phase (versus smoldering), it often lacks correlation with anhydrosugar fragments
14 (e.g., m/z 60), which are more consistent biomass burning markers across burn and fuel types
15 (Lee et al., 2010; Sullivan et al., 2008).

16 PMF factors are mass-spectrally static; to explore the behavior of and variability within each type
17 of OA, periods dominated by a given factor were subjected to elemental, size, and meteorological
18 analyses which will be presented below. "LV-dominated" periods are indicated when $[\text{LV}] \geq$
19 $2*[\text{SV}]$, "SV-dominated" periods when $[\text{SV}] > [\text{LV}]$, and "BBOA-dominated" episodes when
20 $[\text{BB}] \geq 2*0.46 \mu\text{g}/\text{m}^3$ (twice the average BBOA factor concentration).

21 3.3 Elemental Analysis and Organic Nitrogen

22 The ratio of organic mass to organic carbon (OM:OC) averages 1.99 ± 0.16 and indicates highly
23 oxidized OA consistent with other non-urban sites (Aiken et al., 2008; Turpin & Lim, 2001); O:C
24 averages 0.66 ± 0.13 and H:C averages 1.27 ± 0.09 . N:C is determined from CHN and CHON
25 fragments, excluding nominally inorganic fragments such as NO_2^+ that may also arise from
26 fragmentation of organic nitrogen (ON) molecules; N:C averages 0.01 ± 0.01 (max = 0.55).

27 On the van Krevelen-triangle diagram (Fig. 6Error! Reference source not found.), the data
28 position in the apex of the 'ambient triangle' space (higher O:C and lower H:C) indicates highly
29 oxidized particles consistent with similar datasets (Ng et al. 2011; Heald et al. 2010); data points
30 are colored by the dominant PMF factor as defined above. SV-OOA- and BBOA-dominated

ms 10/22/14 6:49 PM

Deleted: Figure

ms 10/22/14 4:39 PM

Deleted: ;

ms 10/22/14 6:49 PM

Deleted: Figure

1 periods occupy similar ranges, while LV-OOA-dominated periods are more oxidized with lower
2 H:C. During BBOA-dominated periods, O:C ranges from ~0.2 to ~0.65, which is a greater range
3 than often observed in the literature (usually ~0.3-0.4, Aiken et al., 2007, 2008; Heringa et al.,
4 2012); the higher maximum degree of oxygenation may arise from the ubiquity of OOA at the
5 site, and/or from additional partitioning of oxidized organics onto the new biomass burning
6 particles. The total dataset also demonstrates consistent high oxidation (i.e. there are no points in
7 the 'HOA/POA' region of the graph indicated by a grey ellipse). The overlap in van Krevelen
8 space between data points from high-concentration LV- and SV-OOA episodes and the
9 concomitance of SV- and LV-OOA time-series ($r^2 = 0.59$) suggest that, *purely in terms of*
10 *oxidation*, SV- and LV-OOA are somewhat arbitrary delineations between air masses whose
11 aerosol oxidation state varies continuously. However, the different inorganic mixtures (and
12 particle sizes, Section 3.4) associated with LV-OOA and SV-OOA validate treating them
13 separately. Linear regressions of O:C/H:C are sometimes used to investigate oxidation
14 mechanisms (Heald et al., 2010). While the reaction mechanisms producing these slopes are best
15 constrained when observing air masses isolated during reaction, a doubtful assumption for this
16 lengthy ambient dataset, these values are provided for reference in the supplement.
17 Quantification of organic nitrogen from AMS data is prevented by fragmentation of ON to
18 nominally inorganic fragments (NO_n^+), the inconsistency of this fragmentation between
19 instruments, and the vast array of possible ON parent compounds in ambient particles (Farmer et
20 al., 2010). However, a lower bound on organic nitrogen mass can be estimated using $\text{ON}_{\min} =$
21 $(\text{Org}/\text{OM}:\text{OC}) * \text{N}:\text{C} * (14/12)$ where 'Org' is total organic mass; ON mass may be underestimated
22 using this method because N:C includes only N from CHON and CHN fragments, disregarding
23 NO_n^+ and/or NH_n^+ produced by ON fragmentation. ON_{\min} is small and comprised mostly of CHN
24 fragments (max = $1.04 \mu\text{g}/\text{m}^3$; average = $0.02 \pm 0.02 \mu\text{g}/\text{m}^3$). The few, modest ON_{\min} events are
25 accompanied by BBOA (although not all BBOA increases are accompanied by ON_{\min}) and total
26 nitrate with no commensurate sulfate or ammonium increases (Fig. 7); ON such as nitrophenols
27 (Iinuma et al., 2007), urea (Mace et al., 2003), nitriles, and amines/amides (Simoneit et al., 2003)
28 have been associated with biomass burning in the literature. Although the half-width/half-max
29 fitting rule was always maintained, CHN fragments are often neighbor to larger organic fragment
30 peaks, which generally complicates identification or quantification of the smaller peak; however,
31 our assertion that these fragments represent real CHN content is supported by contemporaneous,

ms 10/22/14 4:40 PM

Deleted: Aiken et al., 2007;

ms 10/22/14 4:41 PM

Deleted: the

ms 10/22/14 4:42 PM

Deleted: Supplementary

ms 10/22/14 4:42 PM

Deleted: Material

ms 10/22/14 6:49 PM

Deleted: Figure

1 co-located filter-based measurements of water-soluble organic nitrogen, which was enhanced
2 during biomass-burning episodes and contained organic bases, as observed here (Benedict, 2012).
3 Though fragmentation in the AMS precludes identification of parent organic molecules, series of
4 CHN fragments at m/z s 30 and 58 (with additional peaks at m/z s 72, 86, and 100) have been
5 observed in 70eV mass spectra from laboratory and field aerosols with amine content (Murphy et
6 al., 2007; Silva et al., 2008); CH_4N^+ (m/z 30) may result from amine re-arrangement after electron
7 impact ionization (Murphy et al., 2007). Here, prominent CHN fragments are noted at m/z s 30,
8 41, 53, 58, 63, 67, 77, 79, 81, 91, and 95 and are organized into the ‘wave’ pattern often seen in
9 organic spectra (m/z s 53, 67, 81, and 95, ‘Series 1’ in Fig. 8), which arises from the tendency of
10 organic molecules to lose CH_2 groups sequentially during fragmentation and results in peaks
11 separated by 14 amu. Empirical formulae at m/z s 53, 67, 81, and 95 belong overwhelmingly to
12 nitrile and/or pyrrole (heterocyclic) molecules, suggesting that these are (or fragment from)
13 important ON compounds in the local particulate matter; however, because a mixture of amine
14 compounds is possible, molecular structure cannot be determined through fragmentation ratios.
15 Fragments at m/z s 63, 77, and 91 form another methylene-subtraction series (‘Series 2,’ Fig. 8),
16 for which empirical formulae also suggest nitriles and/or heterocyclic compounds, including
17 pyridine, which is often used to stabilize agricultural fertilizers and is produced in small amounts
18 in biomass burning (McKenzie et al., 1995).
19 This CHN series, while not found in the literature, is similar to fragments observed in a similar
20 high-altitude site near Grand Teton National Park (m/z s 30, 41, 55, 58, 67, 79, 91; Schurman,
21 2014). The average CHN mass spectrum for elevated- ON_{min} periods (not shown) has higher CHN
22 signal than average total, LV-OOA, and SV-OOA spectra, but no appreciable difference in
23 fragment patterns, indicating a concentration increase but likely minimal change in CHN
24 composition. The concurrence of increases in ON_{min} and BBOA suggests that ON content, and
25 especially nitrile and/or hetero-aromatics, is enhanced in biomass burning plumes. Although
26 CHON fragments (nominally, ‘organonitrates’) were fit in the high-resolution analysis, they
27 contained very little mass and no clear fragmentation patterns.

28 3.4 Particle Size

29 While low particle concentrations and therefore signal prevent continuous size determination for
30 many observed species (notably inorganics), size determination of marker m/z s and time periods

ms 10/22/14 6:49 PM

Deleted: Figure

ms 10/22/14 6:49 PM

Deleted: Figure

1 heavily dominated by a given organic factor can elucidate ‘average’ particle behavior and perhaps
2 atmospheric processing as discussed below. Lognormal fits of average aerosol component mass
3 size distributions allow better statistical comparison of factor-dominated periods and were
4 constructed using the Igor fitting algorithm; lognormal fits also allow size mode estimation in
5 species such as ammonium and nitrate that suffer from lower signal:noise in the raw size
6 distributions.

7 High-LV-OOA events have larger particles (~380 nm geometric mean diameter) than SV-OOA
8 episodes (~300 nm), while BBOA may be slightly smaller (~280 nm, Fig. 9). As indicated by σ_g
9 (the geometric sd), LV-OOA events are also more monodisperse than SV-OOA; the tendency of
10 condensation and coagulation during oxidation to make particles larger and more monodisperse
11 suggests that the OOA factors spend time in transit from their source (Seinfeld & Pandis, 2006),
12 and further that LV-OOA particles undergo more oxidative processing than SV-OOA particles, as
13 mean radius is observed to increase continuously with ageing (Reid et al., 2005).

14 The similar size distributions and time-series of LV-OOA, ammonium, and sulfate suggest that an
15 internal mixture of these components is common. While SV-OOA and LV-OOA are often
16 coincident, SV-OOA-dominated periods feature smaller particle sizes and a correlation with
17 ammonium nitrate. As mentioned earlier, differences in atmospheric processing of the given
18 components may lead to these distinct mixtures. SV-OOA and ammonium nitrate, all semivolatile
19 species, may arise in the particle phase through condensation of vapors. In contrast, the
20 correlation between LV-OOA and sulfate suggests a possible common aqueous production route.
21 Size distributions of cloud/fog-processed particles tend to be larger than observed here (Hering &
22 Friedlander, 1982; Meng & Seinfeld, 1994), but many of these studies feature heavy, prolonged
23 cloud/fog cover and meteorology and chemistry (e.g. higher aerosol precursor concentrations)
24 which may differ from brief convective cloud processing in the Front Range. Aqueous reactions
25 in wetted particles are also feasible; the deliquescence relative humidity of mixed ammonium
26 sulfate-organic particles is ~30-70% (depending on organic fraction and type) and the ambient
27 surface RH varied from 4-100% during this study with an average of $59 \pm 31\%$ (Smith et al.,
28 2012; Takahama et al., 2007). These RH values are consistent with the historical July-August
29 average RH of ~50%, based on monthly-average data (during 1991-2012, CIRA 2013).

30 BBOA events are smaller and more polydisperse than other organic factors, higher in amplitude,
31 and not coincident with inorganic species, reflecting a fresher, local particle population given less

ms 10/22/14 6:49 PM

Deleted: Figure

ms 10/22/14 4:44 PM

Deleted: td. dev.

ms 10/22/14 4:47 PM

Deleted: the

ms 10/22/14 4:46 PM

Deleted: ; this is

1 time to grow by condensation and/or coagulation. With an average organic mode of ~280 nm, the
2 biomass burning aerosol at this site is consistent with fresh BB plumes from temperate forests,
3 which range in volume mean diameter from 86-300 nm (volume and mass distributions being
4 analogous assuming constant density; Reid et al., 2005 and references therein). 2-D time and size
5 images for some BBOA events at RMNP (not shown) reveal growth of total organics from 100-
6 200 nm to ~350 nm over the course of the event, consistent with observations in the literature and
7 explained by rapid coagulation and condensation (Adler et al., 2011). The level of oxidation
8 (average $f_{44} = 0.09 \pm 0.02$ during BB-dominated periods) is consistent with literature SV-OOA;
9 together, the relatively large size (in comparison to some biomass combustion, e.g. mode = 100
10 nm in Adler et al. 2011, though mode may vary with burn type) and advanced oxidation may be
11 explained by the presence of 'background' OOA and/or rapid condensation of semivolatile VOCs
12 onto the increased particle surface area provided by the BB plume.

13 **3.4 Source/Transport Analysis**

14 The particle composition and size data indicate that oxidized organic aerosol is mixed in varying
15 combinations with inorganic anthropogenic tracers nitrate, sulfate, and ammonium. The level of
16 oxidation argues for prolonged reaction time in the atmosphere; also, limited local habitation
17 precludes high local emissions of inorganic anthropogenic tracers. Together, these suggest
18 transported, anthropogenically-influenced OOA particles, which could arise from either
19 anthropogenic OA and SOA precursors, and/or anthropogenic OA and oxidation products of
20 biogenic organics, such as BVOC oxidation in the presence of NO_x (Kiendler-Scharr et al., 2009).
21 Correlations between secondary OA mass and temperature may indicate which precursors and
22 mechanisms are at play: in many urban/downwind ambient observations, a negative correlation
23 arises from thermodynamically-driven partitioning effects, but in heavily forested areas,
24 increased SOA-precursor BVOC emissions from increasing temperature can overwhelm
25 thermodynamic partitioning reduction, causing an overall increase in secondary mass (Leaith et
26 al., 2011). These studies are usually episode-focused and establish the connectivity of the
27 measured air masses using meteorology and anthropogenic trace gases; at Rocky Mountain, the
28 average relationship between temperature and SOA concentration is determined for periods with
29 up-slope and down-slope winds. Concentrations of LV-OOA, SV-OOA, 'SOA' (defined here as
30 LV+SV), and BBOA have no relationship with ambient temperature during either upslope or

1 downslope winds ($r^2=0.00$, $m=0.00$); this could a) indicate a balance, on average, between
2 thermodynamic partitioning and BVOC precursor emission effects on SOA mass, and/or b) be a
3 product of the inconsistent lag between wind direction and concentration changes (see below).
4 Fragmentation within the AMS prevents the molecular specificity needed to determine which of
5 these mechanisms is at play. However, co-located carbon isotope work conducted in a year with
6 total burned area and fire contributions to surface $PM_{2.5}$ similar to that herein indicates that ~88%
7 of summer $PM_{2.5}$ carbon is contemporary (Schichtel et al., 2008; Val Martin et al., 2013). From
8 the PMF factors, biomass burning OA (which contains contemporary carbon) contributes a study
9 average of ~11% of submicron OC. Thus, biomass burning does not appear to provide all of the
10 observed contemporary C. This suggests that biogenic VOCs may contribute substantially to
11 local OA formation. Levin et al. (2012) described particle growth from condensation of organics
12 in summer at a similar forested Colorado site; concomitant size increase and κ (hygroscopicity
13 parameter) decrease during particle formation events is an indicator of organic condensation.
14 Associating meteorology with component concentrations and diurnal patterns supports these
15 source indications. Surface winds are funneled by the valley topography and are predominantly
16 down-valley from the WNW (48%) or up-valley from the SE (16%); this pattern is consistent
17 inter-annually, with similar wind roses produced by data from 1995-2005 (Malm et al., 2009a).
18 Raw and directionally averaged concentrations of aerosol components plotted against surface
19 wind direction over sixteen $22^\circ 30'$ wind direction bins are shown with conditional probability
20 functions (CPFs) in Fig. 10. High inorganic concentrations are associated with local SE winds
21 indicating up-valley movement from the Front Range and are very similar in both CPF value and
22 meteorological association to co-located $PM_{2.5}$ measurements (note that CPFs are multiplied by
23 10 to share a scale with concentration; Benedict et al. 2013b). CPFs for OOA factors also have an
24 association with southeasterly winds, and higher average concentrations are associated with S-SE
25 winds for all components (including BBOA, though from a different source; see below).
26 However, unlike organics, OOA factors also have above-average concentrations associated with
27 NW winds (though not above the CPF threshold). This may indicate regional OOA content (i.e.
28 “background” organics), possibly aged biogenic SOA from forest emissions, which could
29 originate from the west and be unassociated with Front Range emissions; aqueous processing in
30 orographic clouds arising from westerly flow over the mountains could also contribute to this
31 oxidized OA.

ms 10/22/14 6:49 PM

Deleted: Figure

1 High BBOA concentrations are usually associated with NW or SW-to-S surface winds. The
2 closest campfire source is ~200m WNW of the sampling site; the shorter transport (and therefore
3 dilution) time may explain the higher concentrations in BBOA events from the WNW. Three
4 other camps are placed ~0.5-1 km due south; the increased number and distance of the fires
5 explains the higher average but lower maximum concentrations associated with SW-to-S winds.

6 3.5 Episode Analysis

7 The aerosol characteristics summarized previously are demonstrated in a series of alternating
8 high- and low-concentration periods during July 7-11, which clearly show the transport of OOA
9 and inorganics by SE surface winds (Fig. 11). Initiation of SE flow is followed by marked
10 concentration increases after ~3 hours, suggesting a 3-hour transport time between the Front
11 Range and RMNP during this period. A similar lag applies between down-valley flow initiation
12 and concentration decreases; the fact that 1-3 hour offsets did not improve correlation between
13 wind direction and species concentrations indicates that transport time is, not surprisingly,
14 variable. The abrupt decreases in all components' concentrations following NW wind initiation
15 reveals the relative cleanliness of the air coming over the mountains during these periods. Lastly,
16 note the apparent discrepancy during period A, where ~NW winds are accompanied by sharp
17 spikes in SV-OOA; this is thought to be an entanglement of BBOA mass with SV-OOA (Section
18 3.2) as evidenced by the short, high-amplitude concentration increase, enhancement of m/z 60 in
19 the mass spectrum (not shown), and lack of attendant increase in anthropogenic inorganics. This
20 hypothesis is corroborated by an increase in BBOA in the recombinant-factor PMF analysis (not
21 shown) and the NW placement of the campfire source (as winds are from the north).

ms 10/22/14 6:49 PM

Deleted: Figure

ms 10/22/14 4:48 PM

Deleted: :

ms 10/22/14 4:48 PM

Deleted: this

22 4. Summary and Conclusions

23 The ambient submicron aerosol at the Rocky Mountain National Park ROMO site during 2 July -
24 31 August 2010 is low in average concentration (total average $PM_{10} = 5.13 \pm 2.72 \mu\text{g}/\text{m}^3$),
25 dominated by highly oxidized organics (LV-OOA and SV-OOA), and punctuated by short
26 biomass burning (BBOA) episodes. Mixtures of LV-OOA with ammonium sulfate and SV-OOA
27 with ammonium nitrate are indicated by consistent size distributions and time-series correlation.
28 Inorganic species (nitrate, sulfate, and ammonium) are established anthropogenic emission tracers
29 for which no strong local sources are apparent; high inorganic concentrations are concurrent with

1 southeasterly surface winds that indicate upslope flow from the Front Range. A biogenic
2 contribution, possibly from oxidation of BVOCs as Front Range oxidant-rich pollution plumes
3 are transported over forest, is suggested by the fact that contemporary carbon contributed by local
4 biomass burning may not account for total contemporary carbon at the site (though datasets are
5 not contemporaneous, Schichtel et al., 2008). Organic nitrogen fragments are associated with
6 BBOA and may indicate amine, nitrile, and/or heterocyclic aromatic content, but are low in mass
7 (omitting nominally inorganic fragments from ON calculations); BBOA is not correlated with any
8 measured inorganic species.

9 Transport of oxidized organic aerosols from the Front Range is indicated by advanced oxidation
10 and relative monodispersity (both indicative of ageing), association with inorganic anthropogenic
11 tracers, and concentration correlation with surface upslope flow from the urban and agriculture
12 emissions-rich Front Range; the presence of sulfate, periodic high relative humidity and cloud
13 cover, larger particle sizes, and advanced oxidation of the LV-OOA suggest possible contributions
14 from aqueous processing, while growth by vapor condensation is more likely for SV-
15 OOA/ammonium nitrate particles. A local BBOA source is suggested by biomass combustion
16 markers (m/z s 60 and 73) limited to brief, high-concentration, polydisperse events (suggesting
17 fresh combustion emission), association with local S or NW winds consistent with campfire
18 locations, and an unequivocal diurnal maximum at 22:00 LST, when campfires were set at
19 adjacent summer camps.

20 Lastly, the particle characteristics and sources determined here appear to be typical of summer
21 conditions at the Rocky Mountain site, based on the historical meteorological patterns,
22 IMPROVE (total $PM_{2.5}$, sulfate, nitrate, ammonium, and OC), PILS-IC ($PM_{2.5}$ sulfate, nitrate,
23 and ammonium), filter ($PM_{2.5}$ sulfate, nitrate, and ammonium), and fire (burned area, contribution
24 to surface $PM_{2.5}$) data analyzed here.

25 **Author Contributions**

26 T. L. and M. I. S. conducted field experiments; Y. S. and T. L. consulted during data analysis; B.
27 A. S., S. M. K., and J. L. C., Jr. designed the field campaign and provided support and conceptual
28 guidance; and M. I. S. performed data analysis and wrote the manuscript. All authors collaborated
29 on data interpretation and provided continual feedback during the writing process.

30 **Acknowledgements**

1 This study was supported by NPS #H237009400. We would like to thank Amy Sullivan, Christian
2 Carrico, Katherine Benedict, and Ezra Levin for their extensive support in the field, and the
3 Salvation Army High Peak Camp for site access and logistical assistance.

4 **References**

- 5 Adler, G., Flores, J. M., Abo Riziq, a., Borrmann, S., & Rudich, Y. (2011). Chemical, physical,
6 and optical evolution of biomass burning aerosols: a case study. *Atmospheric Chemistry and*
7 *Physics*, *11*(4), 1491–1503. doi:10.5194/acp-11-1491-2011
- 8 Aiken, A. C., DeCarlo, P. F., & Jimenez, J. L. (2007). Elemental analysis of organic species with
9 electron ionization high-resolution mass spectrometry. *Analytical Chemistry*, *79*(21), 8350–
10 8. doi:10.1021/ac071150w
- 11 Aiken, A. C., Decarlo, P. F., Kroll, J. H., Worsnop, D. R., Huffman, J. A., Docherty, K. S.,
12 Ulbrich, I. M., Mohr, C., Kimmel, J. R., Sueper, D., Sun, Y., Zhang, Q., Trimborn, A.,
13 Northway, M., Ziemann, P. J., Canagaratna, M. R., Onasch, T. B., Alfarra, M. R., Prevot, A.
14 S. H., Dommen, J., Duplissy, J., Metzger, A., Baltensperger, U., Jimenez, J. L. (2008). O/C
15 and OM/OC ratios of primary, secondary, and ambient organic aerosols with high-resolution
16 time-of-flight aerosol mass spectrometry. *Environmental Science & Technology*, *42*(12),
17 4478–85.
- 18 Alfarra, M. R., Prevot, A. S. H., Szidat, S., Sandradewi, J., Weimer, S., Lanz, V. A., Schreiber,
19 D., Mohr, M., Baltensperger, U. (2007). Identification of the mass spectral signature of
20 organic aerosols from wood burning emissions. *Environmental Science & Technology*,
21 *41*(16), 5770–7.
- 22 Baron, J. S., Rueth, H. M., Wolfe, A. M., Nydick, K. R., Allstott, E. J., Minear, J. T., & Moraska,
23 B. (2000). Ecosystem responses to nitrogen deposition in the Colorado Front Range.
24 *Ecosystems*, *3*(4), 352–368.
- 25 Barth, M. C., Rasch, P. J., Kiehl, J. T., Benkovitz, C. M., & Schwartz, S. E. (2000). Sulfur
26 chemistry in the National Center for Atmospheric Research Community Climate Model:
27 Description, evaluation, features, and sensitivity to aqueous chemistry. *Journal of*
28 *Geophysical Research*, *105*(D1), 1387. doi:10.1029/1999JD900773
- 29 Benedict, K. B. (2012). *Observations of Atmospheric Reactive Nitrogen Species and Nitrogen*
30 *Deposition in the Rocky Mountains*. Colorado State University, Fort Collins, CO.
- 31 Benedict, K. B., Carrico, C. M., Kreidenweis, S. M., Schichtel, B., Malm, W. C., & Collett, J. L.
32 (2013). A seasonal nitrogen deposition budget for Rocky Mountain National Park.
33 *Ecological Applications*, *23*(5), 1156–1169. doi:10.1890/12-1624.1

- 1 Benedict, K. B., Day, D., Schwandner, F. M., Kreidenweis, S. M., Schichtel, B., Malm, W. C., &
2 Collett, J. L. (2013). Observations of atmospheric reactive nitrogen species in Rocky
3 Mountain National Park and across northern Colorado. *Atmospheric Environment*, 64(null),
4 66–76. doi:10.1016/j.atmosenv.2012.08.066
- 5 Bossert, J. E., & Cotton, W. R. (1994). Regional-Scale Flows in Mountainous Terrain. Part I: A
6 Numerical and Observational Comparison. *Monthly Weather Review*, 122(7), 1449–1471.
7 doi:10.1175/1520-0493(1994)122<1449:RSFIMT>2.0.CO;2
- 8 Chan, Y., Hawas, O., Hawker, D., Vowles, P., Cohen, D. D., Stelcer, E., Simpson, R., Golding,
9 G., Christensen, E. (2011). Using multiple type composition data and wind data in PMF
10 analysis to apportion and locate sources of air pollutants. *Atmospheric Environment*, 45(2),
11 439–449. doi:10.1016/j.atmosenv.2010.09.060
- 12 Chen, Q., Farmer, D. K., Schneider, J., Zorn, S. R., Heald, C. L., Karl, T. G., Guenther, A., Allan,
13 J. D., Robinson, N., Coe, H., Kimmel, J. R., Pauliquevis, T., Borrmann, S., Pöschl, U.,
14 Andreae, M. O., Artaxo, P., Jimenez, J. L., Martin, S. T. (2009). Mass spectral
15 characterization of submicron biogenic organic particles in the Amazon Basin. *Geophysical*
16 *Research Letters*, 36(20), L20806. doi:10.1029/2009GL039880
- 17 CIRA. (2013). VIEWS Database. Retrieved January 22, 2014, from
18 <http://views.cira.colostate.edu/web/>
- 19 Corrigan, A. L., Russell, L. M., Takahama, S., Äijälä, M., Ehn, M., Junninen, H., ... Williams, J.
20 (2013). Biogenic and biomass burning organic aerosol in a boreal forest at Hyytiälä, Finland,
21 during HUMPPA-COPEC 2010. *Atmospheric Chemistry and Physics*, 13(24), 12233–12256.
22 doi:10.5194/acp-13-12233-2013
- 23 Decarlo, P. F., Kimmel, J. R., Trimborn, A., Northway, M. J., Jayne, J. T., Aiken, A. C., Gonin,
24 M., Fuhrer, K., Horvath, T., Docherty, K. S., Worsnop, D. R., Jimenez, J. L. (2006). Field-
25 deployable, high-resolution, time-of-flight aerosol mass spectrometer. *Analytical Chemistry*,
26 78(24), 8281–9. doi:10.1021/ac061249n
- 27 Echalar, F., Gaudichet, A., Cachier, H., & Artaxo, P. (1995). Aerosol emissions by tropical forest
28 and savanna biomass burning: Characteristic trace elements and fluxes. *Geophysical*
29 *Research Letters*, 22(22), 3039. doi:10.1029/95GL03170
- 30 Farmer, D. K., Matsunaga, A., Docherty, K. S., Surratt, J. D., Seinfeld, J. H., Ziemann, P. J., &
31 Jimenez, J. L. (2010). Response of an aerosol mass spectrometer to organonitrates and
32 organosulfates and implications for atmospheric chemistry. *Proc. Natl. Acad. Sci.*, 107,
33 6670–6675.
- 34 Gebhart, K. A., Schichtel, B. A., Malm, W. C., Barna, M. G., Rodriguez, M. A., & Collett, J. L.
35 (2011). Back-trajectory-based source apportionment of airborne sulfur and nitrogen

- 1 concentrations at Rocky Mountain National Park, Colorado, USA. *Atmospheric*
2 *Environment*, 45(3), 621–633. doi:10.1016/j.atmosenv.2010.10.035
- 3 Hand, J. L., Schichtel, B. A., Pitchford, M., Malm, W. C., & Frank, N. H. (2012). Seasonal
4 composition of remote and urban fine particulate matter in the United States. *Journal of*
5 *Geophysical Research*, 117(D5), D05209. doi:10.1029/2011JD017122
- 6 Heald, C. L., Kroll, J. H., Jimenez, J. L., Docherty, K. S., DeCarlo, P. F., Aiken, A. C., Chen, Q.,
7 Martin, S. T., Farmer, D. K., Artaxo, P. (2010). A simplified description of the evolution of
8 organic aerosol composition in the atmosphere. *Geophysical Research Letters*, 37(8),
9 L08803. doi:10.1029/2010GL042737
- 10 Hering, S. V., & Friedlander, S. K. (1982). Origins of aerosol sulfur size distributions in the Los
11 Angeles basin. *Atmospheric Environment*, 16(11), 2647–2656. doi:10.1016/0004-
12 6981(82)90346-8
- 13 Heringa, M. F., DeCarlo, P. F., Chirico, R., Tritscher, T., Clairotte, M., Mohr, C., ...
14 Baltensperger, U. (2012). A new method to discriminate secondary organic aerosols from
15 different sources using high-resolution aerosol mass spectra. *Atmospheric Chemistry and*
16 *Physics*, 12(4), 2189–2203. doi:10.5194/acp-12-2189-2012
- 17 Iinuma, Y., Brüggemann, E., Gnauk, T., Müller, K., Andreae, M. O., Helas, G., Parmar, R.,
18 Herrmann, H. (2007). Source characterization of biomass burning particles: The combustion
19 of selected European conifers, African hardwood, savanna grass, and German and
20 Indonesian peat. *Journal of Geophysical Research*, 112(D8), D08209.
21 doi:10.1029/2006JD007120
- 22 Jimenez, J. L., Canagaratna, M. R., Donahue, N. M., Prevot, A. S. H., Zhang, Q., Kroll, J. H.,
23 DeCarlo, P. F., Allan, J. D., Coe, H., Ng, N. L., Aiken, A. C., Docherty, K. S., Ulbrich, I.
24 M., Grieshop, A. P., Robinson, A. L., Duplissy, J., Smith, J. D., Wilson, K. R., Lanz, V. A.,
25 Hueglin, C., Sun, Y. L., Tian, J., Laaksonen, A., Raatikainen, T., Rautiainen, J., Vaattovaara,
26 P., Ehn, M., Kulmala, M., Tomlinson, J. M., Collins, D. R., Cubison, M. J., Dunlea, E. J.,
27 Huffman, J. A., Onasch, T. B., Alfarra, M. R., Williams, P. I., Bower, K. N., Kondo, Y.,
28 Schneider, J., Drewnick, F., Borrmann, S., Weimer, S., Demerjian, K. L., Salcedo, D.,
29 Cottrell, L. D., Griffin, R. J., Takami, A., Miyoshi, T., Hatakeyama, S., Shimojo, A., Sun, J.
30 Y., Zhang, Y. M., Dzepina, K., Kimmel, J. R., Sueper, D., Jayne, J. T., Herndon, S. C.,
31 Trimborn, A. M., Williams, L. R., Wood, E. C., Middlebrook, A. M., Kolb, C. E.,
32 Baltensperger, U., Worsnop, D. R. (2009). Evolution of organic aerosols in the atmosphere.
33 *Science (New York, N.Y.)*, 326(5959), 1525–9. doi:10.1126/science.1180353
- 34 Kiendler-Scharr, A., Zhang, Q., Hohaus, T., Kleist, E., Mensah, A., Mentel, T. F., Spindler, C.,
35 Uerlings, R., Tillmann, R., Wildt, J. (2009). Aerosol mass spectrometric features of biogenic
36 SOA: observations from a plant chamber and in rural atmospheric environments.
37 *Environmental Science & Technology*, 43(21), 8166–72. doi:10.1021/es901420b

- 1 Kim, E., & Hopke, P. K. (2004). Comparison between Conditional Probability Function and
2 Nonparametric Regression for Fine Particle Source Directions. *Atmospheric Environment*,
3 38(28), 4667–4673. doi:10.1016/j.atmosenv.2004.05.035
- 4 Kroll, J. H., Donahue, N. M., Jimenez, J. L., Kessler, S. H., Canagaratna, M. R., Wilson, K. R.,
5 Altieri, K. E., Mazzoleni, L. R., Wozniak, A. S., Bluhm, H., Mysak, E. R., Smith, J. D.,
6 Kolb, C. E., Worsnop, D. R. (2011). Carbon oxidation state as a metric for describing the
7 chemistry of atmospheric organic aerosol. *Nature Chemistry*, 3(2), 133–9.
8 doi:10.1038/nchem.948
- 9 Lanz, V. A., Alfarra, M. R., Baltensperger, U., Buchmann, B., Hueglin, C., & Prevot, A. S. H.
10 (2007). Source apportionment of submicron organic aerosols at an urban site by factor
11 analytical modelling of aerosol mass spectra. *Atmos. Chem. Phys.*, (2004), 1503–1522.
- 12 Leaitch, W. R., Macdonald, A. M., Brickell, P. C., Liggio, J., Sjostedt, S. J., Vlasenko, A.,
13 Bottenheim, J. W., Huang, L., Li, S.-M., Liu, P. S. K., Toom-Sauntry, D., Hayden, K. A.,
14 Sharma, S., Shantz, N. C., Wiebe, H. A., Zhang, W., Abbatt, J. P. D., Slowik, J. G., Chang,
15 R. Y. W., Russell, L. M., Schwartz, R. E., Takahama, S., Jayne, J. T., Ng, N. L. (2011).
16 Temperature response of the submicron organic aerosol from temperate forests. *Atmospheric*
17 *Environment*, 45(37), 6696–6704. doi:10.1016/j.atmosenv.2011.08.047
- 18 Lee, T., Sullivan, A. P., Mack, L., Jimenez, J. L., Kreidenweis, S. M., Onasch, T. B., Worsnop,
19 D. R., Malm, W. C., Wold, C. E., Hao, W. M., Collett, J. L. (2010). Chemical Smoke
20 Marker Emissions During Flaming and Smoldering Phases of Laboratory Open Burning of
21 Wildland Fuels. *Aerosol Science and Technology*, 44(9), 2635–2643, i–v.
22 doi:10.1080/02786826.2010.499884
- 23 Lelieveld, J., & Heintzenberg, J. (1992). Sulfate Cooling Effect on Climate Through In-Cloud
24 Oxidation of Anthropogenic SO₂. *Science (New York, N.Y.)*, 258(5079), 117–20.
25 doi:10.1126/science.258.5079.117
- 26 Levin, E. J. T., Kreidenweis, S. M., McMeeking, G. R., Carrico, C. M., Collett Jr., J. L., & Malm,
27 W. C. (2009). Aerosol physical, chemical and optical properties during the Rocky Mountain
28 Airborne Nitrogen and Sulfur study. *Atmospheric Environment*, 43(11), 1932–1939.
29 doi:10.1016/j.atmosenv.2008.12.042
- 30 Levin, E. J. T., Prenni, A. J., Petters, M. D., Kreidenweis, S. M., Sullivan, R. C., Atwood, S. A.,
31 Ortega, J., DeMott, P. J., Smith, J. N. (2012). An annual cycle of size-resolved aerosol
32 hygroscopicity at a forested site in Colorado. *Journal of Geophysical Research*, 117(D6),
33 D06201. doi:10.1029/2011JD016854
- 34 Liu, P. S. K., Deng, R., Smith, K. A., Williams, L. R., Jayne, J. T., Canagaratna, M. R., Moore,
35 K., Onasch, T. B., Worsnop, D. R., Deshler, T. (2007). Transmission Efficiency of an
36 Aerodynamic Focusing Lens System: Comparison of Model Calculations and Laboratory

- 1 Measurements for the Aerodyne Aerosol Mass Spectrometer. *Aerosol Science and*
2 *Technology*, 41(8), 721–733. doi:10.1080/02786820701422278
- 3 Mace, K. A., Artaxo, P., & Duce, R. A. (2003). Water-soluble organic nitrogen in Amazon Basin
4 aerosols during the dry (biomass burning) and wet seasons. *Journal of Geophysical*
5 *Research*, 108(D16), 4512. doi:10.1029/2003JD003557
- 6 Malm, W. C., Barna, M. G., Beem, K. B., Carrico, C. M., Collett Jr., J. L., Day, D. E., Gebhart,
7 K.A., Hand, J.L., Kreidenweis, S.M., Lee, T., Levin, E.J.T., McDade, C.E., McMeeking,
8 G.R., Molenaar, J.V., Raja, S., Rodriguez, M. A., Schichtel, B. A., Schwandner, F. M.,
9 Sullivan, A. P., Taylor, C. (2009a). *Rocky Mountain Atmospheric Nitrogen and Sulfur Study*.
10 Fort Collins, CO, Cooperative Institute for Research in the Atmosphere.
- 11 Malm, W. C., McMeeking, G. R., Kreidenweis, S. M., Levin, E. J. T., Carrico, C. M., Day, D. E.,
12 Collett Jr., J. L., Lee, T., Sullivan, A. P., Raja, S. (2009b). Using high time resolution
13 aerosol and number size distribution measurements to estimate atmospheric extinction.
14 *Journal of the Air & Waste Management Association (1995)*, 59(9), 1049–60.
- 15 McKenzie, L. M., Hao, W. M., Richards, G. N., & Ward, D. E. (1995). Measurement and
16 modeling of air toxins from smoldering combustion of biomass. *Environmental Science &*
17 *Technology*, 29(8), 2047–54. doi:10.1021/es00008a025
- 18 Meng, Z., & Seinfeld, J. H. (1994). On the Source of the Submicrometer Droplet Mode of Urban
19 and Regional Aerosols. *Aerosol Science and Technology*, 20(3), 253–265.
20 doi:10.1080/02786829408959681
- 21 Murphy, S. M., Sorooshian, a., Kroll, J. H., Ng, N. L., Chhabra, P., Tong, C., ... Seinfeld, J. H.
22 (2007). Secondary aerosol formation from atmospheric reactions of aliphatic amines.
23 *Atmospheric Chemistry and Physics Discussions*, 7(1), 289–349. doi:10.5194/acpd-7-289-
24 2007
- 25 Ng, N. L., Canagaratna, M. R., Jimenez, J. L., Chhabra, P. S., Seinfeld, J. H., & Worsnop, D. R.
26 (2011). Changes in organic aerosol composition with aging inferred from aerosol mass
27 spectra. *Atmospheric Chemistry and Physics*, 11(13), 6465–6474. doi:10.5194/acp-11-6465-
28 2011
- 29 Ng, N. L., Canagaratna, M. R., Zhang, Q., Jimenez, J. L., Tian, J., Ulbrich, I. M., ... Worsnop, D.
30 R. (2010). Organic aerosol components observed in Northern Hemispheric datasets from
31 Aerosol Mass Spectrometry. *Atmospheric Chemistry and Physics*, 10(10), 4625–4641.
32 doi:10.5194/acp-10-4625-2010
- 33 Orsini, D. A., Ma, Y., Sullivan, A. P., Sierau, B., Baumann, K., & Weber, R. J. (2003).
34 Refinements to the particle-into-liquid sampler (PILS) for ground and airborne
35 measurements of water soluble aerosol composition. *Atmospheric Environment*, 37, 1243–
36 1259.

- 1 Paatero, P., & Tapper, U. (1994). Positive matrix factorization: A non-negative factor model with
2 optimal utilization of error estimates of data values. *Environmetrics*, 5(2), 111–126.
- 3 Parrish, D. D., Hahn, C. H., Fahey, D. W., Williams, E. J., Bollinger, M. J., Hübler, G., Buhr, M.
4 P., Murphy, P. C., Trainer, M., Hsie, E. Y., Liu, S. C., Fehsenfeld, F. C. (1990). Systematic
5 Variations in the Concentration of NO_x (NO Plus NO₂) at Niwot Ridge, Colorado. *Journal*
6 *of Geophysical Research*, 95(D2), 1817–1836. doi:10.1029/JD095iD02p01817
- 7 Reid, J. S., Koppmann, R., Eck, T. F., & Eleuterio, D. P. (2005). A review of biomass burning
8 emissions part II: intensive physical properties of biomass burning particles. *Atmospheric*
9 *Chemistry and Physics*, 5(3), 799–825. doi:10.5194/acp-5-799-2005
- 10 Schichtel, B. A., Malm, W. C., Bench, G., Fallon, S., McDade, C. E., Chow, J. C., & Watson, J.
11 G. (2008). Fossil and contemporary fine particulate carbon fractions at 12 rural and urban
12 sites in the United States. *Journal of Geophysical Research*, 113(D2), D02311.
13 doi:10.1029/2007JD008605
- 14 Schurman, M. I. (2014). *Characteristics, Sources, and Formation of Organic Aerosols in the*
15 *Rocky Mountains*. Colorado State University, Fort Collins, Colorado.
- 16 Seinfeld, J. H., & Pandis, S. N. (2006). *Atmospheric Chemistry and Physics: From Air Pollution*
17 *to Climate Change* (2nd ed., p. 1232). New York: John Wiley & Sons. New York, New
18 York, USA.
- 19 Silva, P. J., Erupe, M. E., Price, D., Elias, J., Malloy, Q. G. J., Li, Q., Warren, B., Cocker, D. R.
20 (2008). Trimethylamine as precursor to secondary organic aerosol formation via nitrate
21 radical reaction in the atmosphere. *Environmental Science & Technology*, 42(13), 4689–96.
- 22 Simoneit, B. R. T., Rushdi, A. I., bin Abas, M. R., & Didyk, B. M. (2003). Alkyl Amides and
23 Nitriles as Novel Tracers for Biomass Burning. *Environmental Science & Technology*,
24 37(1), 16–21. doi:10.1021/es020811y
- 25 Simoneit, B. R. T., Schauer, J. J., Nolte, C. G., Oros, D. R., Elias, V. O., Fraser, M. P., Rogge, W.
26 F., Cass, G. R. (1999). Levoglucosan, a tracer for cellulose in biomass burning and
27 atmospheric particles. *Atmospheric Environment*, 33(2), 173–182. doi:10.1016/S1352-
28 2310(98)00145-9
- 29 Smith, M. L., Bertram, A. K., & Martin, S. T. (2012). Deliquescence, efflorescence, and phase
30 miscibility of mixed particles of ammonium sulfate and isoprene-derived secondary organic
31 material. *Atmospheric Chemistry and Physics Discussions*, 12(4), 9903–9943.
32 doi:10.5194/acpd-12-9903-2012
- 33 Solomon, S., Qin, D., Manning, M., Chen, Z., Marquis, M., Averyt, K. B., Tigora, M., Miller, H.
34 L. (2007). Climate Change 2007: The Physical Science Basis. In *Fourth Assessment Report*

- 1 *of the Intergovernmental Panel on Climate Change*. Cambridge: Cambridge University
2 Press.
- 3 Sullivan, A. P., Holden, A. S., Patterson, L. A., McMeeking, G. R., Kreidenweis, S. M., Malm,
4 W. C., Hao, W. M., Wold, C. E., Collett, J. L. (2008). A method for smoke marker
5 measurements and its potential application for determining the contribution of biomass
6 burning from wildfires and prescribed fires to ambient PM 2.5 organic carbon. *Journal of*
7 *Geophysical Research*, 113(D22), D22302. doi:10.1029/2008JD010216
- 8 Sun, J., Zhang, Q., Canagaratna, M. R., Zhang, Y., Ng, N. L., Sun, Y., Jayne, J. T., Zhang, X.,
9 Zhang, X., Worsnop, D. R. (2010). Highly time- and size-resolved characterization of
10 submicron aerosol particles in Beijing using an Aerodyne Aerosol Mass Spectrometer.
11 *Atmospheric Environment*, 44(1), 131–140. doi:10.1016/j.atmosenv.2009.03.020
- 12 Sun, Y., Zhang, Q., Macdonald, A. M., Hayden, S. K., Li, S. M., Liggio, J., Liu, P. S. K., Anlauf,
13 K. G., Leaitch, W. R., Steffen, A., Cubison, M., Worsnop, D. R., van Donkelaar, A., Martin,
14 R. V. (2009). Size-resolved aerosol chemistry on Whistler Mountain, Canada with a high-
15 resolution aerosol mass spectrometer during INTEX-B. *Atmospheric Chemistry and Physics*,
16 9(9), 3095–3111. doi:10.5194/acp-9-3095-2009
- 17 Takahama, S., Pathak, R. K., & Pandis, S. N. (2007). Efflorescence Transitions of Ammonium
18 Sulfate Particles Coated with Secondary Organic Aerosol. *Environmental Science &*
19 *Technology*, 41(7), 2289–2295. doi:10.1021/es0619915
- 20 Turpin, B. J., & Lim, H.-J. (2001). Species Contributions to PM_{2.5} Mass Concentrations:
21 Revisiting Common Assumptions for Estimating Organic Mass. *Aerosol Science and*
22 *Technology*, 35(1), 602–610. doi:10.1080/02786820119445
- 23 Ulbrich, I. M., Canagaratna, M. R., Zhang, Q., Worsnop, D. R., & Jimenez, J. L. (2009).
24 Interpretation of organic components from Positive Matrix Factorization of aerosol mass
25 spectrometric data. *Atmospheric Chemistry and Physics*, 9(9), 2891–2918. doi:10.5194/acp-
26 9-2891-2009
- 27 Ulbrich, I. M., Canagaratna, M. R., Cubison, M. J., Zhang, Q., Ng, N. L., Aiken, A. C., and
28 Jimenez, J. L. (2012). Three-dimensional factorization of size-resolved organic aerosol mass
29 spectra from Mexico City. *Atmos. Meas. Tech.*, 5, 195–224, doi:10.5194/amt-5-195-2012.
- 30 Val Martin, M., Heald, C. L., Ford, B., Prenni, A. J., & Wiedinmyer, C. (2013). A decadal
31 satellite analysis of the origins and impacts of smoke in Colorado. *Atmospheric Chemistry*
32 *and Physics*, 13(15), 7429–7439. doi:10.5194/acp-13-7429-2013
- 33 Weimer, S., Alfarra, M. R., Schreiber, D., Mohr, M., Prévôt, A. S. H., & Baltensperger, U. (2008).
34 Organic aerosol mass spectral signatures from wood-burning emissions: Influence of
35 burning conditions and wood type. *Journal of Geophysical Research*, 113(D10), 1–10.
36 doi:10.1029/2007JD009309

- 1 Xie, Y., & Berkowitz, C. M. (2007). The use of conditional probability functions and potential
2 source contribution functions to identify source regions and advection pathways of
3 hydrocarbon emissions in Houston, Texas. *Atmospheric Environment*, *41*(28), 5831–5847.
4 doi:10.1016/j.atmosenv.2007.03.049
- 5 Zhang, Q., Alfara, M. R., Worsnop, D. R., Allan, J. D., Coe, H., Canagaratna, M. R., & Jimenez,
6 J. L. (2005). Deconvolution and quantification of hydrocarbon-like and oxygenated organic
7 aerosols based on aerosol mass spectrometry. *Environmental Science & Technology*, *39*(13),
8 4938–52.
- 9 Zhang, Q., Jimenez, J. L., Canagaratna, M. R., Allan, J. D., Coe, H., Ulbrich, I. M., ... Worsnop,
10 D. R. (2007). Ubiquity and dominance of oxygenated species in organic aerosols in
11 anthropogenically-influenced Northern Hemisphere midlatitudes. *Geophysical Research*
12 *Letters*, *34*(13), 1–6. doi:10.1029/2007GL029979
- 13 Zhang, Q., Jimenez, J. L., Canagaratna, M. R., Ulbrich, I. M., Ng, N. L., Worsnop, D. R., & Sun,
14 Y. (2011). Understanding atmospheric organic aerosols via factor analysis of aerosol mass
15 spectrometry: a review. *Analytical and Bioanalytical Chemistry*, *401*(10), 3045–67.
16 doi:10.1007/s00216-011-5355-y
- 17 Zhou, L., Hopke, P. K., Stanier, C. O., Pandis, S. N., Ondov, J. M., & Pancras, J. P. (2005).
18 Investigation of the relationship between chemical composition and size distribution of
19 airborne particles by partial least squares and positive matrix factorization. *Journal of*
20 *Geophysical Research*, *110*(D7), D07S18. doi:10.1029/2004JD005050

1 Table 1. July-August average \pm standard deviation concentrations of particulate species in $\mu\text{g}/\text{m}^3$.
 2 **The IMPROVE network collects 24-hour PM_{2.5} nylon-filter samples for nitrite, nitrate, sulfate,**
 3 **and chloride, and quartz filters for organic matter and elemental carbon analysis.** IMPROVE data
 4 are averaged over July and August during 2005-2012 (“IMPROVE”) or over July and August
 5 during 2010 (“IMPRV 2010”), and were accessed via the VIEWS database on 22 January 2014.
 6 **Bold** text indicates significant difference (using Wilcoxon Rank test) between IMPROVE 2010
 7 and AMS data averaged to the 24-hr IMPROVE time-resolution. *Benedict et al. (2013). **
 8 IMPROVE does not measure ammonium; it is calculated as the amount needed to neutralize
 9 sulfate and nitrate.

ms 10/23/14 7:44 PM

Comment [5]: Table 1 caption, line 2: after "...g m-3." inserted: "The IMPROVE network collects 24-hour PM_{2.5} nylon-filter samples for nitrite, nitrate, sulfate, and chloride, and quartz filters for organic matter and elemental carbon analysis."

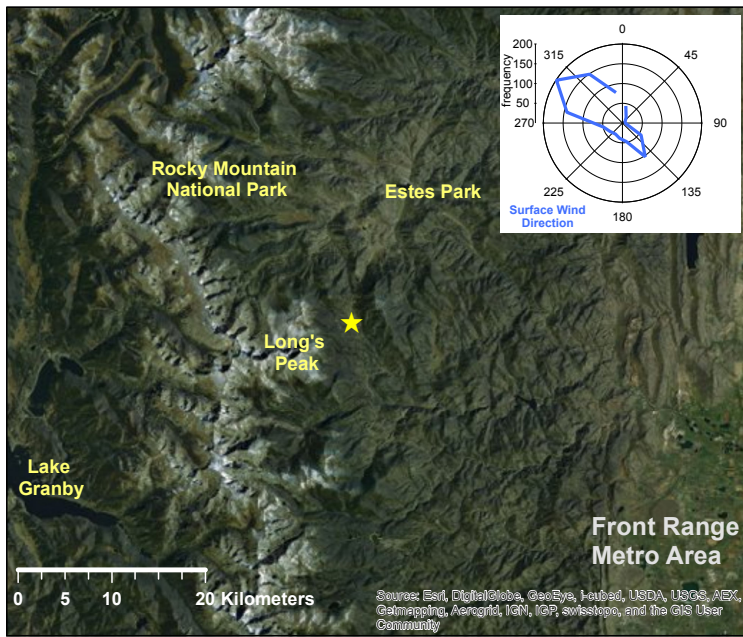
	NO ₃	SO ₄	NH ₄	OM	PM _{2.5}
This study	0.22 \pm 0.24	0.85 \pm 0.48	0.20 \pm 0.14	3.86 \pm 2.66	PM ₁ : 5.13 \pm 2.72
Summer 2006*	0.12	0.99	0.32		
Summer 2010*	0.08 \pm 0.06	0.31 \pm 0.14	0.18 \pm 0.07		
IMPROVE	0.08 \pm 0.10	0.42 \pm 0.19	0.02 \pm 0.03**	3.90 \pm 6.11	5.13 \pm 4.36
IMPRV 2010	0.12 \pm 0.13	0.53 \pm 0.27	0.04 \pm 0.04**	1.48 \pm 0.64	3.13 \pm 1.29

1 | Table 2. Time-series coefficients of determination (r^2) between inorganic species and organic
2 | factors calculated using the IGOR linear regression algorithm.

	LVOOA	SVOOA	BBOA	SO ₄	NO ₃
SO ₄	0.77	0.18	0.05		
NO ₃	0.33	0.41	0.02	0.34	
NH ₄	0.76	0.72	0.03	0.97	0.89

ms 10/23/14 7:45 PM

Deleted: correlation

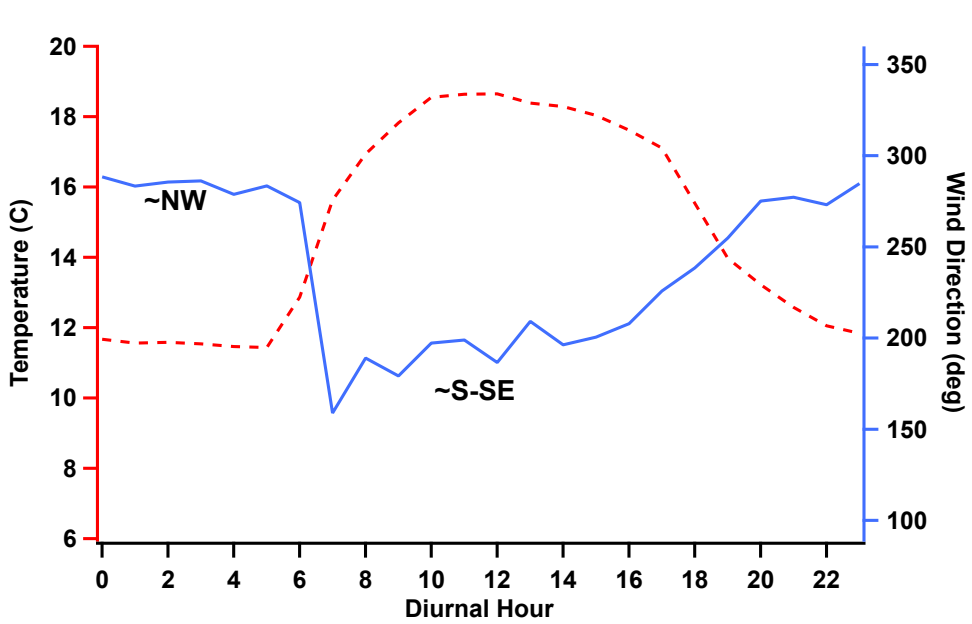


1
2
3
4
5
6

Figure 1. Map showing the Rocky Mountain National Park sampling site (yellow star). Boulder, Denver, and other cities form the Front Range metro area to the east (ARCgis map generation: Zitely Tzompa, 15 March 2014). The wind rose shows a histogram of wind directions measurements during the study.

ms 10/23/14 8:14 PM
Formatted: Don't keep with next, Tabs:Not at 0"

ms 10/23/14 8:14 PM
Deleted: -

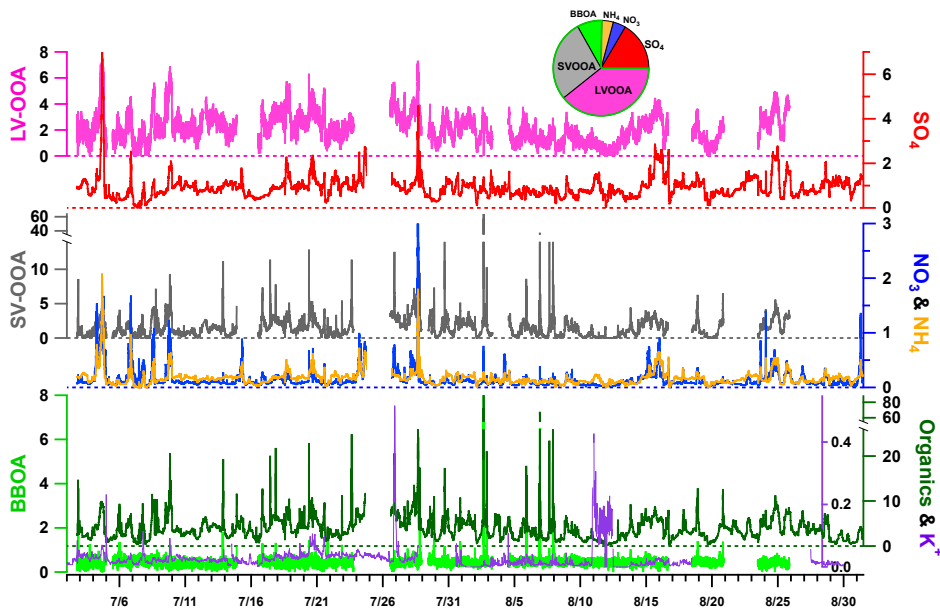


1

2

3 Figure 2. Study-average diurnal variation of ambient temperature (red dashed line, left axis) and

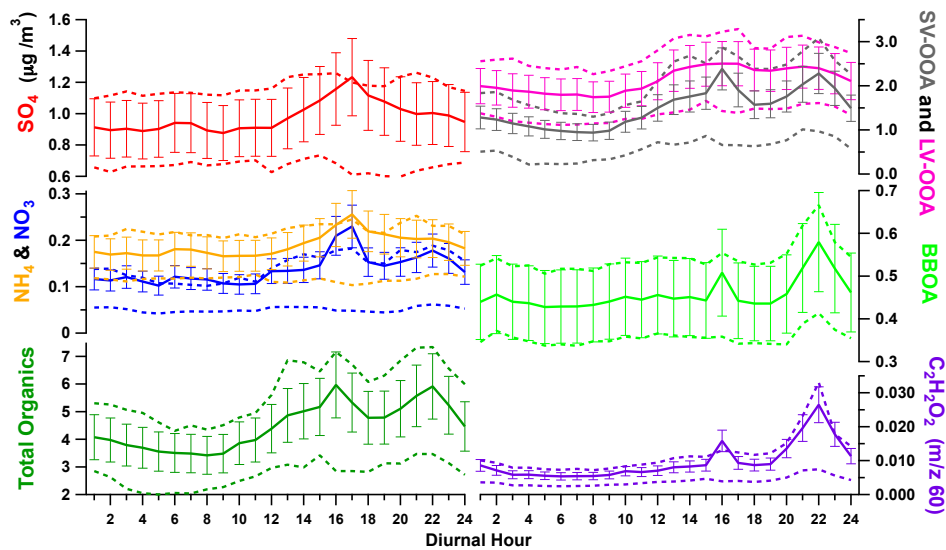
4 surface wind direction (blue line, right axis).



1

2

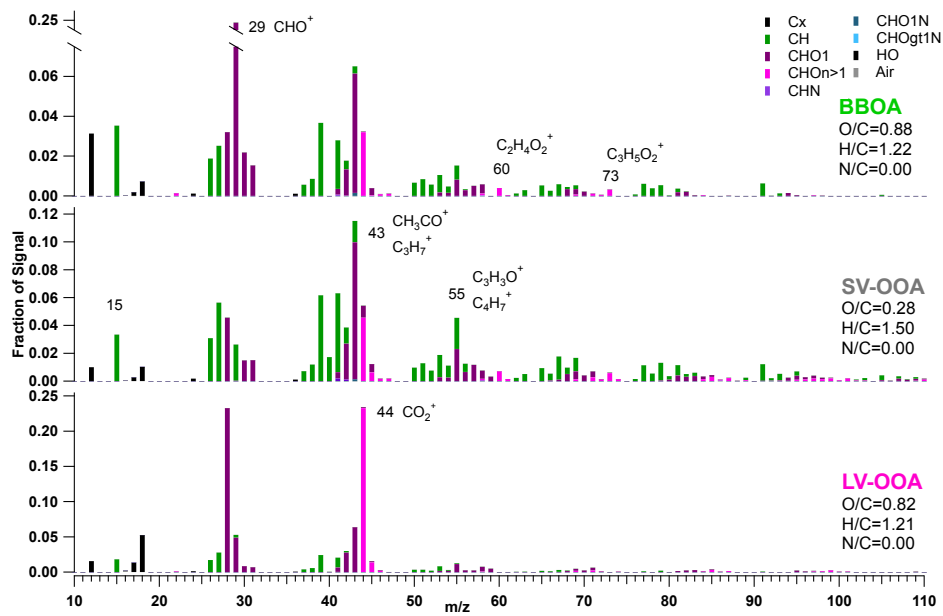
3 Figure 3. Time series of inorganic components, total organics, and organic factors (LV-OOA,
 4 SV-OOA, and BBOA) in $\mu\text{g}/\text{m}^3$. Potassium (K^+) is from 17-minute-average PILS-IC samples. Pie
 5 chart shows study-average contributions for each component; the dark green outline contains total
 6 organics.



1

2

3 Figure 4. Study-average diurnal concentrations of particulate sulfate, nitrate, ammonium, total
 4 organics, BBOA, LV-OOA, SV-OOA, $C_3H_3O^+$ (m/z 55), and $C_2H_4O_2^+$ (m/z 60, levoglucosan).
 5 Solid lines are means, with $\pm 20\%$ error bars reflecting AMS quantitation error. Dashed lines are
 6 25th and 75th percentiles.



1

2

3 **Figure 5.** Normalized mass spectra of organic aerosol types determined by Positive Matrix

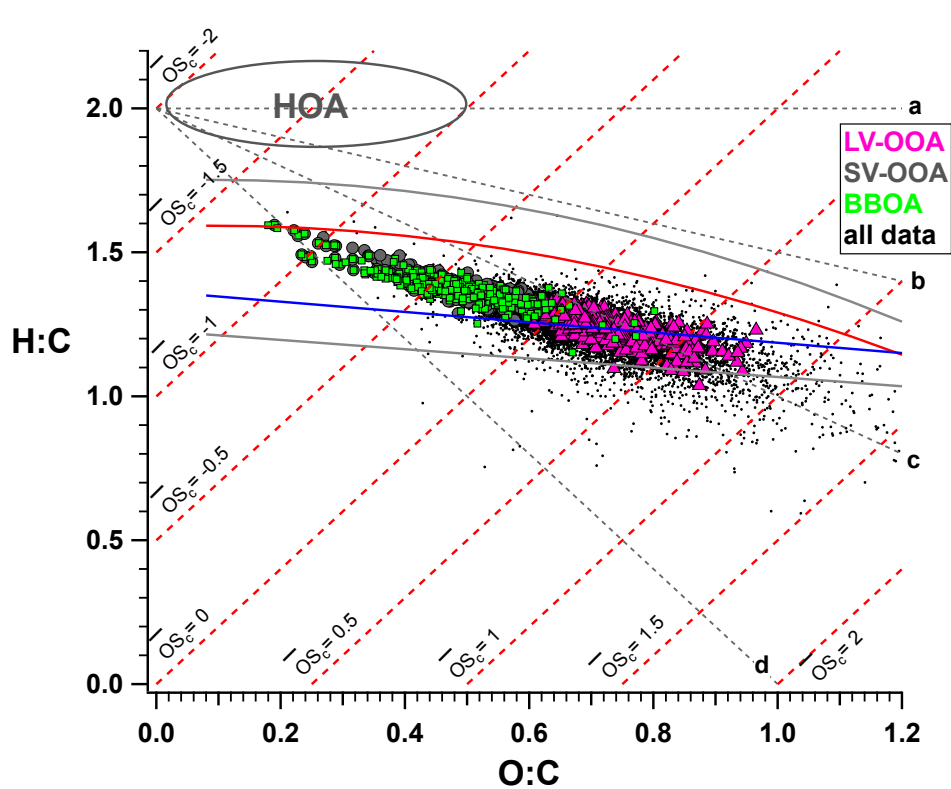
4 Factorization (Paatero and Tapper, 1994): Biomass Burning Organic Aerosol (BBOA), Semi-

5 Volatile Oxidized Organic Aerosol (SV-OOA), and Low Volatility Oxidized Organic Aerosol

6 (LV-OOA). O/C values are calculated for the given factor mass spectrum.

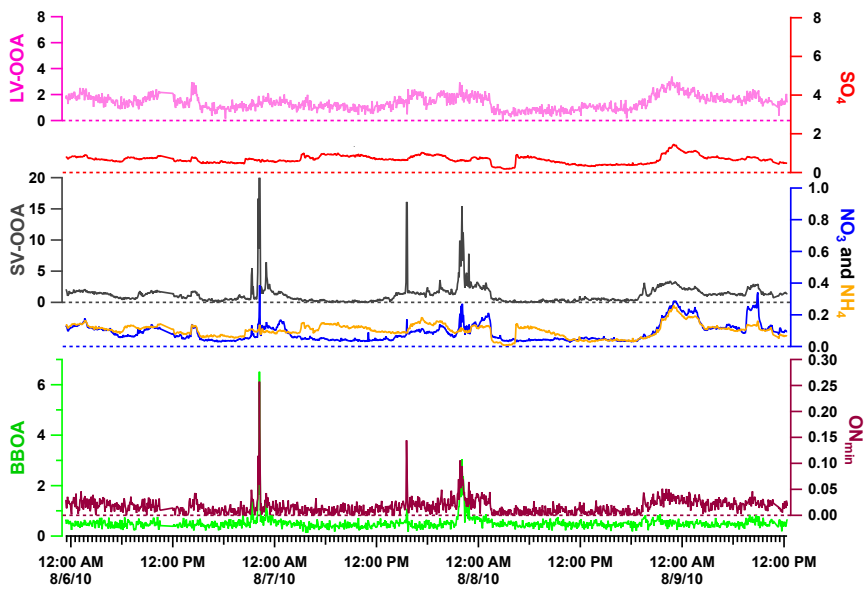
ms 10/23/14 8:21 PM

Comment [6]: Please use figure f05_092714.pdf instead of the previous version of Figure 5. (It just includes a few more elemental analysis details, but is not significantly different)



1
2

3 Figure 6. Van Krevelen-triangle diagram for time periods dominated by the given factor (as
 4 defined in Section 3.3) and for all data points. Estimated oxidation state, $\overline{OS}_c \approx 2 \cdot O:C - H:C$ (Kroll
 5 et al., 2011). Red and blue lines indicate the region usually inhabited by ambient data in the *f43*
 6 vs. *f44* plot; grey lines represent 10% error. Grey ellipse shows typical HOA values. a:
 7 +alcohol/peroxide, $m = 0$; b: carboxylic acid + fragmentation, $m = -0.5$; c: +carboxylic acid (no
 8 fragmentation), $m = -1$; d: +ketone/aldehyde, $m = -2$ (Ng et al. 2011).

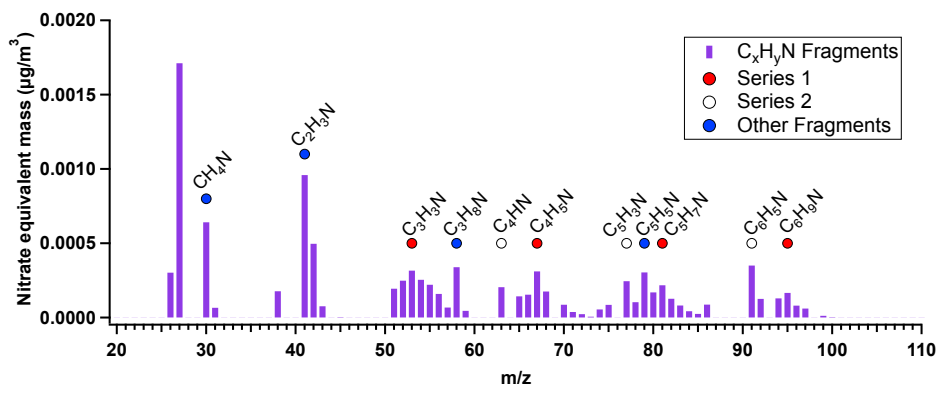


1

2

3 Figure 7. Time series showing select elevated- ON_{min} periods with inorganics and other organic

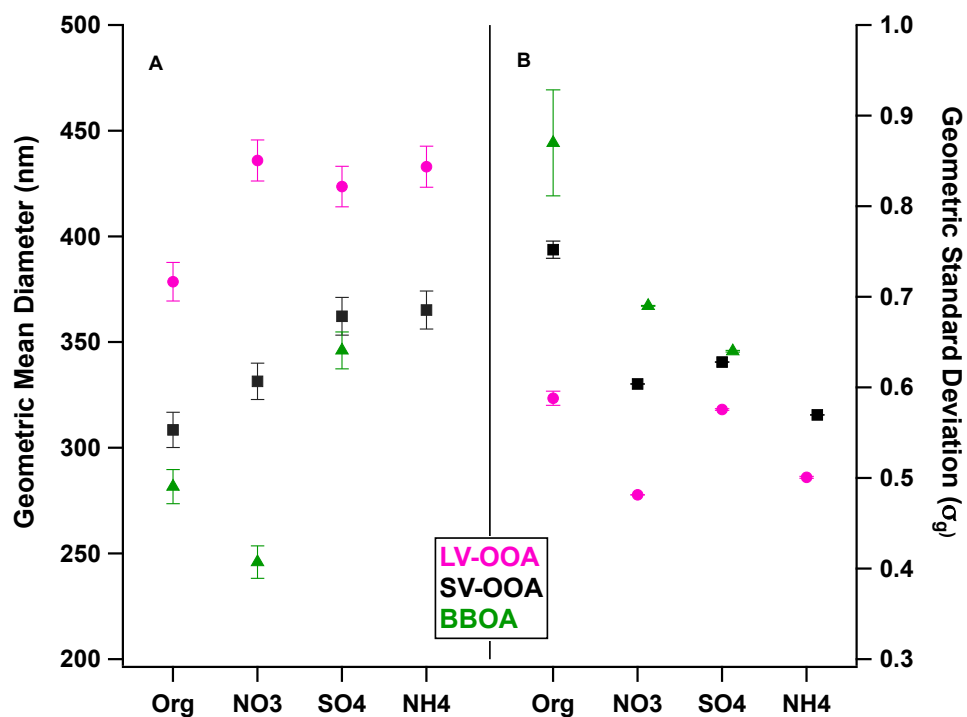
4 factors from the Rocky Mountain National Park site.



1

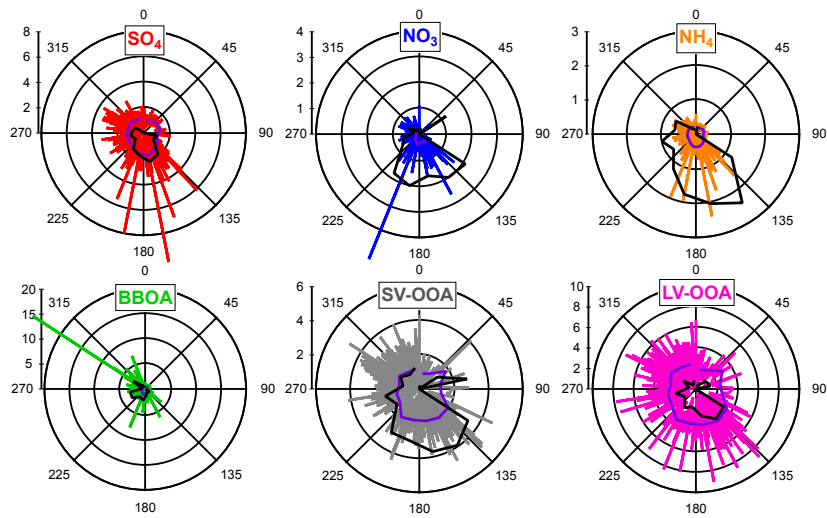
2

3 Figure 8. Rocky Mountain study-average mass spectrum of CHN fragments.



1
2

3 Figure 9. A) Geometric mean diameter of the log normal mass size distribution fit for the
 4 indicated species or total organics for the average of time periods dominated by the color-
 5 designated organic factor; error bars are estimations of size-dependent PToF error, compounding
 6 chopper broadening and calibration-particle size standard deviation (Supplement). B) Geometric
 7 standard deviation of the lognormal fit, with error bars equaling the reduced chi-squared value.
 8 Ammonium concentrations were too low during BBOA events for size determination.



1

2

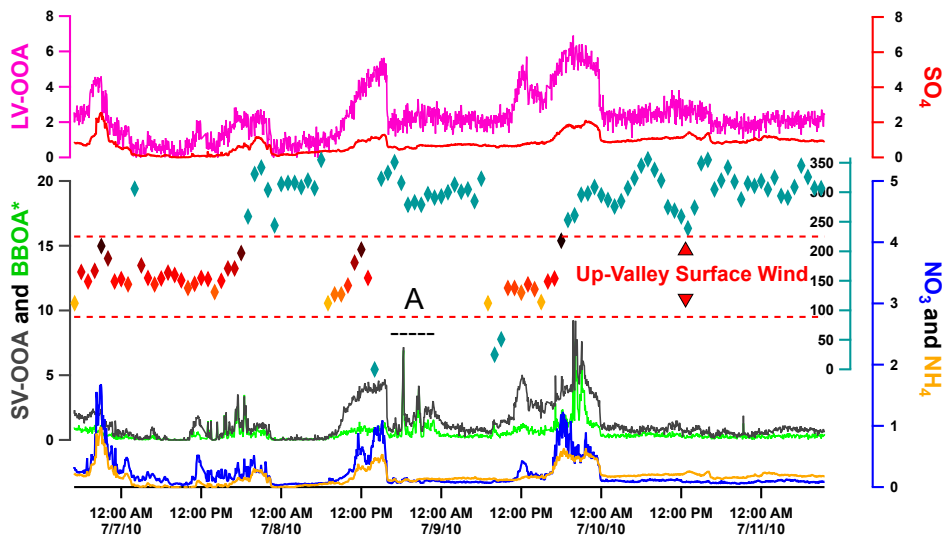
3 Figure 10. 1-hour average concentrations ($\mu\text{g}/\text{m}^3$) of organic aerosol types with surface wind
 4 direction. Raw data are colored by species; average concentrations over the sixteen $22^\circ30'$ wind
 5 direction bins are shown in purple; and black lines indicate the Conditional Probability Function
 6 (CPF multiplied by 10).

ms 10/22/14 4:52 PM

Deleted: .

ms 10/22/14 4:52 PM

Deleted: .



1
2

3 Figure 11. Timeline of species and relevant organic factor concentrations for 7-11 July 2010,
 4 plotted with 1-hour surface wind direction at the site (diamonds). Wind directions 90 through 180
 5 degrees denote up-valley winds and are demarcated by dashed red lines and warm-colored
 6 diamonds. BBOA* is calculated using the six-factor PMF reconstructions outlined in the
 7 supplement.

ms 10/22/14 4:52 PM
 Deleted: teal